International Journal of Nanomedicine

Dovepress
open access to scientific and medical research

Open Access Full Text Article

ORIGINAL RESEARCH

Gold nanoparticles reduce high glucose-induced oxidative-nitrosative stress regulated inflammation and apoptosis via tuberin-mTOR/NF-κB pathways in macrophages

This article was published in the following Dove Press journal:
International Journal of Nanomedicine
17 August 2017
Number of times this article has been viewed

Huma Rizwan[1]
Jagdeep Mohanta[2]
Satyabrata Si[1,2]
Arttatrana Pal[3]

[1]School of Biotechnology, KIIT University, Bhubaneswar, India; [2]School of Applied Sciences, KIIT University, Bhubaneswar, India; [3]Department of Zoology, School of Life Sciences, Mahatma Gandhi Central University, Bihar, India

Abstract: Hyperglycemia is a risk factor for cardiovascular mortality and morbidity, and directly responsible for exacerbating macrophage activation and atherosclerosis. We showed that gold nanoparticles (AuNPs) reduce the high glucose (HG)-induced atherosclerosis-related complications in macrophages via oxidative-nitrosative stress-regulated inflammation and apoptosis. The effects of AuNPs on oxidative-nitrosative stress markers such as cellular antioxidants were attenuated by HG exposure, leading to reduction in the accumulation of reactive oxygen/nitrogen species in cellular compartments. Further, these abnormalities of antioxidants level and reactive oxygen/nitrogen species accumulations initiate cellular stress, resulting in the activation of nuclear factor κB (NF-κB) via ERK1/2mitogen-activated protein kinase (MAPK)/Akt/tuberin-mammalian target of rapamycin (mTOR) pathways. The activated NF-κB stimulates inflammatory mediators, which subsequently subdue biomolecules damage, leading to aggravation of the inflammatory infiltration and immune responses. Treatment of AuNPs inhibits the intracellular redox-sensitive signaling pathways, inflammation, and apoptosis in macrophages. Together, our results indicate that AuNPs may modulate HG-induced oxidative-nitrosative stress. These effects may be sealed tight due to the fact that AuNPs treatment reduces the activation of NF-κB by ERK1/2MAPK/Akt/tuberin-mTOR pathways-mediated inflammatory genes expression and cellular stress responses, which may be beneficial for minimizing the atherosclerosis.

Keywords: gold nanoparticles, oxidative-nitrosative stress, apoptosis, macrophages, atherosclerosis

Introduction

Hyperglycemia is a risk factor for cardiovascular complications and directly responsible for exacerbating atherosclerosis.[1] Our previous study demonstrated that high glucose (HG) exposure to macrophages triggered increase in free oxygen/nitrogen radicals in cellular compartments.[2] HG-induced reactive oxygen/nitrogen species (ROS/RNS) overproduction may be a key event in activation of signaling pathways involved in the pathogenesis of atherosclerosis.[2,3] Interestingly, the mechanism of autoxidation describes the capability of glucose to enolize, thereby reducing molecular oxygen and yielding oxidizing intermediates, including superoxide anion ($O_2^{\bullet-}$), hydroxyl radical (•OH), and hydrogen peroxide (H_2O_2), all of which can damage membrane lipids, proteins and nucleic acids through cross-linking and fragmentation.[4,5] Macrophages play an important role in arterial relaxation because they produce nitric oxide (NO).[6] Accumulation of NO acts as a potent nitrovasodilator and modulates vascular tone.[7]

Correspondence: Arttatrana Pal
Department of Zoology, School of Life Sciences, Mahatma Gandhi Central University, East Champarun, Motihari, Bihar, 845401, India
Email arttatranapal@mgcub.ac.in

submit your manuscript | www.dovepress.com
Dovepress
http://dx.doi.org/10.2147/IJN.S141839

On the other hand, $O_2^{\bullet-}$ was implicated in the physiological inactivation of NO, however, the reaction between $O_2^{\bullet-}$ and NO yields peroxynitrite (ONOO−), a powerful oxidizing agent and potent initiator of DNA single-strand breakage.[8,9] When macrophages respond to HG, ROS/RNS production was increased in cellular compartments and these reactive species triggered DNA strand breakage, leading to rapid increase in amounts of 8-hydroxydeoxyguanosine (8-OHdG) in DNA and decreases in the amount of DNA repair enzyme 8-oxoguanine glycosylase (OGG1).[2] Recent studies have revealed that HG-induced cellular changes lead to alterations of signal transduction cascades in macrophages, affecting gene expression and protein functions both in mitochondria and nuclei. More importantly, both mitochondria and nuclei are 2 main targets of oxidative-nitrosative stress that contain different types of DNA repair enzymes.[4] In this context, apoptosis occurs when the endogenous antioxidants and DNA repair systems are overwhelmed with oxidative-nitrosative overload and cannot overcome the damages inflicted to the cells, including macrophages in different disease conditions.[4,10]

Our recent studies reveal that the regulation of nuclear factor κB (NF-κB) expression was redox sensitive.[4] More importantly, ROS/RNS generated by HG in macrophages may represent key intermediates in the regulation of NF-κB expression. Also, evidence linking the HG-induced oxidative-nitrosative stress with phosphorylation of Akt and ERK1/mitogen-activated protein kinase (2MAPK) in macrophages, additionally supports a role of these kinases in the control of NF-κB expression.[2] Many studies have demonstrated that antioxidants and Akt/ERK1/2 inhibitors abolished HG-induced Akt/ERK1/2 expression in macrophages, thus implicating ROS/RNS and kinases as signaling molecules in this effect.[3,11] Ferenbach et al[12] demonstrated that resident kidney cells and infiltrating monocytes secreted the pro-inflammatory mediators such as cytokines, chemokines and growth factors in response to hyperglycemia. Recent publications have revealed that release of cytokines, including tumor necrosis factor-α (TNF-α)-, interleukin-6, and interleukin-1β due to hyperglycemia further aggravated the inflammatory infiltration and immune responses in the pathology of diabetic complications in macrophages.[2]

Gold nanoparticles (AuNPs) are known from centuries ago as coloring agents and medicines. More importantly, AuNPs have a strong interaction with light called surface plasmon resonance, which is further modulated with shape, size and surrounding medium. Owing to their unique opto-electronic properties, AuNPs have been widely used in biomedical applications, like sensing, imaging, drug delivery and therapeutic agents, besides other applications like, catalysis, electronic devices, energy conversion, etc.[13] The antioxidative effect of traditional gold in treatment of inflammatory diseases has affirmed the urge for study on the restorative effect of AuNPs in diabetes, which has not yet been revealed. There is a great possibility for their interaction with macrophages and to influence atherosclerosis.[14,15] The inhibitory effect of AuNPs against oxidative-nitrosative stress and inactivation of NF-κB that deregulates the expression of diverse inflammatory mediators and immune response genes are lacking. The present study aims to understand the basic mechanism and pathways of inhibitory activity of AuNPs on HG-induced ROS/RNS production, antioxidant depletion, biomolecules damage, inflammation and apoptosis, which is explained by phosphorylation of NF-κB via ERK1/2MAPK/Akt/tuberin-mammalian target of rapamycin (mTOR) pathways in macrophages.

Methods

Materials

Hydrogen tetrachloroaurate(III) trihydrate ($HAuCl_4.3H_2O$), trisodium citrate ($Na_3C_6H_5O_7$), propidium iodide (PI), D-glucose, 5,5-dithiobis(2-nitrobenzoic acid), and MTT were purchased from Sigma Aldrich (St Louis, MO, USA). DMEM, Roswell Park Memorial Institute 1640 (RPMI-1640) medium and fetal bovine serum (FBS) were obtained from Gibco (Invitrogen, Carlsbad, CA, USA). Phorbol-12-myristate-13-acetate was obtained from MP Biomedicals (Santa Ana, CA, USA). Dihydroethidium (DHE), dihydrorodamine 123 (DHR), 2′,7′-dichlorodihydrofluorescein diacetate (CM-H_2DCFDA), and 4,6-diamidino-2-phenylindole (DAPI) were purchased from Molecular probes (Eugene, OR, USA). Neutral red was purchased from Himedia, Mumbai, India. The phosphorylated and total ERK1/2, Akt, tuberin, mTOR, H2A.X, IκBα, p65, cytochrom C, caspases, proliferating cell nuclear antigen (PCNA), chk1, chk2, cyclin A, cyclin B1, cdc2, P53, β-actin and horseradish peroxidase (HRP)-conjugated secondary antibodies were obtained from Cell Signaling Technology (Danvers, MA, USA). Antibodies against OGG1 and 8-OHdG were from Abcam (Cambridge, UK), whereas superoxide dismutase (SOD) was purchased from IMGENEX, Bhubaneswar, India.

Synthesis, characterization of AuNPs and protein corona assay

The citrate-stabilized AuNPs were prepared by Turkevich synthesis approach with minor modification.[16] Briefly,

$HAuCl_4 \cdot 3H_2O$ 5 mL (5 mM) solution was diluted with 44 mL of distilled water and kept stirring under heating. Once the solution started boiling, 1 mL (30 mM) of $Na_3C_6H_5O_7$ was added and the entire solution turned blue followed by wine red color. The heating was stopped and stirring kept on until the solution attained room temperature. The volume of the solution was adjusted with distilled water, filtered to separate any solid impurities, and used as it was for further characterization and experimentation. For ultraviolet-visible (UV-Vis) spectra, the prepared AuNPs were taken in a 1 cm path length quartz cuvette and measured the absorption spectra (Agilent Cary 60 UV-Vis; USA). The transmission electron microscopy (TEM) (Hitachi H-7650 TEM; Elk Grove Village, IL, USA) images were recorded on an accelerating voltage of 120 kV by putting about 10 µL of the prepared water dispersion samples onto a carbon-coated 400 mesh copper grid. The protein corona formation assay was performed as described previously.[17] Briefly, the ability of the serum proteins to bind AuNPs was evaluated using sodium dodecyl sulfate polyacrylamide gel electrophoresis (SDS-PAGE) and Coomassie staining.

Cell culture and treatments

Murine macrophage (RAW264.7) and human monocytic (THP-1) cells were purchased from the National Centre For Cell Science (NCCS), Pune, India, and cultured in medium containing 5 mM D-glucose, and 10% FBS. THP-1 cells were treated with phorbol myristate acetate (20 nmol/L) for differentiation into the adherent macrophages. As per the experimental need, cells were sub-cultured with/without additional glucose (25 mM) followed by different concentrations of AuNPs (1, 5, 10 and 20 nM) for 24 h.

Measurements of antioxidants and ROS/RNS

The antioxidant activity assays were carried out as described previously.[18–20] To measure the ROS, nitrotetrazolium blue reduction assay was carried out as described previously.[2] Intracellular $O_2^{\bullet -}$ production was measured by using the DHE dye as described previously.[4] Briefly, cells were cultured in HG for 24 h with/without AuNPs, trypsinized, washed, and suspended in PBS containing DHE (5 µM) for 30 min at 37°C. Then, 10,000 events per sample were examined for fluorescence in the fluorescein isothiocyanate (FITC) channel by fluorescence-activated cell sorting (FACS) analyzer (Becton Dickinson, San Jose, CA, USA). The •OH level was determined as described previously.[21] Briefly, treated cells were harvested and 300 µL (80 g protein) cell lysate was mixed with 700 µL of PBS solutions (0.1 M EDTA, 2 mM sodium salicylate, 40 µL 10 N HCl and 0.25 g NaCl). Subsequently, an equal volume of ice cold diethyl ether was added, incubated for 30 min at 25°C and absorbance was recorded at 510 nm. Next, CM-H_2DCFDA dye was used to determine the level of intracellular H_2O_2.[22] NO was determined by measuring the nitrite production. Briefly, 100 µL of culture media was mixed with 100 µL Griess reagent and absorbance was recorded at 520 nm. Intracellular $ONOO^-$ production was measured by using the DHR probes as described previously.[11] For microscopic analysis, cells were cultured onto glass coverslips, stained with DHE/DHR for ROS/RNS and fixed with 3.7% paraformaldehyde. The glass cover slip was mounted on glass slides and observed under a microscope (Olympus BX61; Rockville, MD, USA).

Estimation of biomolecules damage

For the determination of lipid peroxidation (LPO), 0.002% butylated hydroxytoluene was mixed with 80 µg of protein samples and incubated at 37°C for 1 h. Thiobarbituric acid solution (0.375%) was added to the above solution followed by centrifugation at 800× *g*. The solution was kept in a boiling water bath for 15 min, and absorbance was recorded.[23] For the determination of protein carbonylation (PC), 80 µg (450 µL) protein samples were mixed with 450 µL of PBS, 100 µL of 10% streptomycin sulfate, and centrifuged at 1,000× *g* for 10 min. Then, 400 µL of the supernatant was mixed with an equal volume of 10 mM 2,4-dinitrophenylhydrazine and kept for 30 min in the dark. Ice-cold trichloroacetic acid (20%) was added to the reaction mixture and centrifuged at 1,000× *g*. The pellet was dissolved in 6 M guanidine hydrochloride and absorbance was recorded.[23] Comet assay was carried out as described previously.[23] The DNA ladder assay was carried out as described previously.[11]

Apoptosis, cell cycle and lysosomal staining

Cell proliferation inhibitory effect of AuNPs on HG-treated cells was evaluated by MTT assay. Briefly, macrophage cells were cultured in 96-well plates with/without HG in the presence/absence of AuNPs. Then, MTT reagent, 20 µL of 5 mg/mL was added, and the plate was incubated in the dark for another 4 h. The solution was removed, and the remaining crystals were solubilized with dimethyl sulfoxide and incubated for an additional 10 min with gentle shaking before the measurement of absorbance. For DAPI staining, after desired treatment, cells were washed with PBS and fixed in 3.7% paraformaldehyde for 20 min. Then, cells were centrifuged at 2,000× *g* for 5 min before staining with DAPI (5 µg/mL) solution.

For Hoechst staining, after desired treatments, cells were incubated with the Hoechst stains, and washed thoroughly with PBS. Then, the slides were mounted with cover slips and photographed immediately. For the cell cycle analysis, treated cells were harvested, pelleted down, resuspended in PI solution and analyzed by FACS analyzer. The number of apoptotic cells was measured by annexin-V FITC by flow cytometry as described previously.[11] Lysosomal staining was carried out by the method of Mytych et al.[24] Briefly, after desired treatment as indicated above, Neutral Red (0.001%) was added and incubated at 37°C for 3 h. The cells were fixed in formaldehyde (0.5%) in 1% $CaCl_2$ solution for 20 min at room temperature, washed with water and examined under fluorescence microscope (FLoid Cell Imaging Station; Life Technologies, Grand Island, NY, USA).

Immunoblotting

RAW264.7 cells were exposed to HG followed by different concentrations of AuNPs. After incubation for 24 h, the cells were harvested, lysed with lysis buffer and protein concentration was determined by Bradford assay.[11] Further, 40–60 µg protein samples were electrophoresed on 8%–12% SDS-PAGE and transferred onto polyvinylidine difluoride membranes. After blocking with fat-free skim milk, membranes were incubated overnight with primary antibodies (1:1,000) followed by incubation with HRP-conjugated secondary antibody (1:2,000) and the protein bands were detected with an enhanced chemiluminescence (ECL™ Plus). The same membrane was reprobed with anti-β-actin antibody as a loading control.

Immunocytochemistry

RAW264.7 cells were cultured on glass coverslips and treated with/without HG in the presence/absence of AuNPs for 24 h.[22] Cells were fixed with 4% paraformaldyhyde followed by blocking with 1% bovine serum albumin and incubated with anti-NF-κB, anti-OGG1 and anti-8-OHdG antibodies followed by FITC-conjugated secondary antibody. FITC green signals were detected by using a fluorescence microscope.

Quantitative real-time polymerase chain reaction (qRT-PCR)

After desired treatment, total RNA of RAW264.7 cells was extracted by using TRIzol (Invitrogen). The cDNA was prepared using Revert Aid cDNA synthesis kit (Thermo Scientific, Grand Island, NY, USA) and qPCR was performed with a CFX connect Real-Time system (BIO-RAD, Hercules, CA, USA) by using KAPA SYBR® FAST qPCR Kit (KAPA Biosystems, Inc., Wilmington, MA, USA) and Oligonucleotides (Table S1).

Statistical analysis

All the statistical analyses were performed using GraphPad Prism (GraphPad Software, Inc., La Jolla, CA, USA). Statistical significance was evaluated using analysis of variance followed by Student's *t*-test. A significance level of $P<0.05$ was considered to be statistically significant. All experiments were performed 3–4 times and expressed as the mean ± standard error of the mean (SEM).

Results

Synthesis of citrate stabilized AuNPs

The citrate-stabilized AuNPs of size below 20 nm were prepared under reflux condition. Formation of AuNPs resulted in a color change of the solution from light yellow to wine red color in boiling aqueous solution. The citrate ions in boiled condition reduce Au(III) ion to Au(0) followed by crystal growth resulting in the formation of defined size Au-nanocrystals, which get stabilized by citrate ions present in the solution. The resultant AuNPs showed a sharp surface plasmon band at 528 nm in the UV-Vis spectrum (Figure 1A). The size of the AuNPs was found to be ~25 nm, as calculated from the UV-Vis absorption spectra using the theory put forth by Haiss et al.[25] According to Mie theory, the appearance of plasmon band position at 528 nm further supports the formation of AuNPs in this size regime. A representative TEM image of the said AuNPs is shown in Figure 1B. The size of the citrate-stabilized AuNPs and the corresponding size distribution was evaluated using the ImageJ software (NIH, Bethseda, MD, USA) (Figure 1C). The average size of the AuNPs was calculated to be 16±1.3 nm taking into consideration at least 50 particles into the count with a very narrow size distribution. The size calculated from TEM images was different from that calculated from UV-Vis absorption spectrum. The difference arises due to the use of the approximation put forth by Haiss et al,[25] which was only applicable for particles above 20 nm diameters. Then, we used AuNPs to understand the inhibitory effect of HG-induced oxidative-nitrosative stress-regulated biomolecules damage and apoptosis in macrophages. Therefore, the binding ability of serum proteins present in cell culture medium to the surface of AuNPs was determined, when 15 mL culture medium was concentrated and subjected to protein corona analysis after 24 h treatment with 5 µg/mL AuNPs. As shown in Figure 1D, there was no evidence that short-term incubation with AuNPs in culture medium considerably affected the tendency for agglomeration.

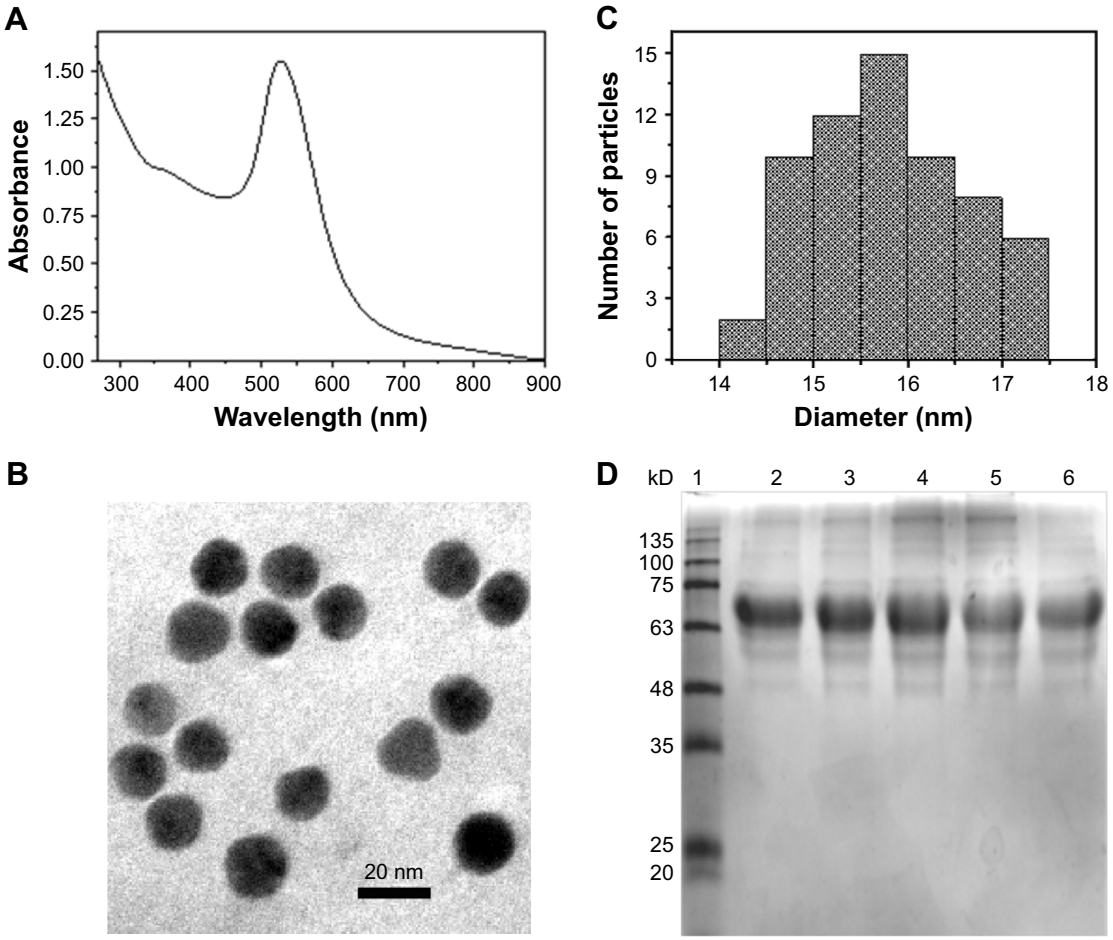

Figure 1 Synthesis and characterization of citrate-stabilized AuNPs.
Notes: (**A**) UV-Vis absorption spectrum of AuNPs showing SPR band. (**B**) TEM image of AuNPs and (**C**) corresponding size distribution of AuNPs. (**D**) The binding ability of serum proteins to the surface of AuNPs. Lane 1-protein ladder, lane 2-DMEM with 10% FBS, lane 3-PBS with 10% FBS, lane 4-DMEM with 10% FBS and HG (25 mM), lane 5-DMEM with 10% FBS and AuNPs (20 nM), and lane 6-DMEM with 10% FBS, HG and AuNPs (20 nM). All experiments were performed three to four times and expressed as the mean ± standard error of the mean.
Abbreviations: UV-Vis, ultraviolet-visible; AuNPs, gold nanoparticles; TEM, transmission electron microscopy; FBS, fetal bovine serum; HG, high glucose; SPR, surface plasmon resonance.

AuNPs treatment improves the HG-induced antioxidants depletion in macrophages

To see the effect of AuNPs on HG-induced antioxidants level, RAW264.7 cells were treated with HG followed by different concentrations of AuNPs. It was observed that dose-dependent treatment of AuNPs restored the SOD level in HG-exposed cells (Figure 2A and B). Further, we checked the expression of specific mitochondrial Mn-SOD and cytosolic Cu-Zn-SOD. As shown in Figure 2C and D, Mn-SOD/Cu-Zn-SOD was increased in HG treated cells and pretreatment with AuNPs attenuated the Mn-SOD/Cu-Zn-SOD level in RAW264.7 cells. Thereafter, we measured the effect of AuNPs on catalase (CAT) level in RAW264.7 cells treated with HG. Spectrophotometer assay showed the increased activity of CAT in HG-exposed cells, but AuNPs restored the activity dose-dependently (Figure 2E). To further confirm the increased activity of CAT in HG exposure and attenuation by AuNPs, we measured the mRNA expression of CAT antioxidant by qRT-PCR. As shown in Figure 2F, the increased expression of CAT antioxidant after HG exposure decreased after AuNPs treatment. Similarly, the level of glutathione peroxidase (GPx) was reduced after HG exposure, but dose-dependent treatment of AuNPs restored the activity in RAW264.7 cells (Figure 2G). Also, the mRNA expression of GPx was decreased after HG exposure, and the activity was restored after treatment with 10 and 20 nM AuNPs (Figure 2H). Next, we measured the reduced glutathione (GSH) level with/without treatment of AuNPs in HG-treated RAW264.7 cells. The GSH level was reduced in HG-exposed cells and treatment with AuNPs restored the GSH level in a dose-dependent manner (Figure 2I).

Inhibitory effect of AuNPs on HG-induced ROS and RNS production in macrophages

We studied the inhibitory effect of AuNPs on HG-induced ROS production in macrophages. The macrophage cells were treated with increasing concentrations of AuNPs in the presence/absence of HG. We observed that HG exposure enhanced the O_2·– production in macrophages and dose-dependent treatment of AuNPs attenuated the O_2·– production (Figure 3A and B). FACS analysis and fluorescence microscopy also confirmed the inhibitory effect of AuNPs (Figure 3C–E). Further, we measured the inhibitory effect

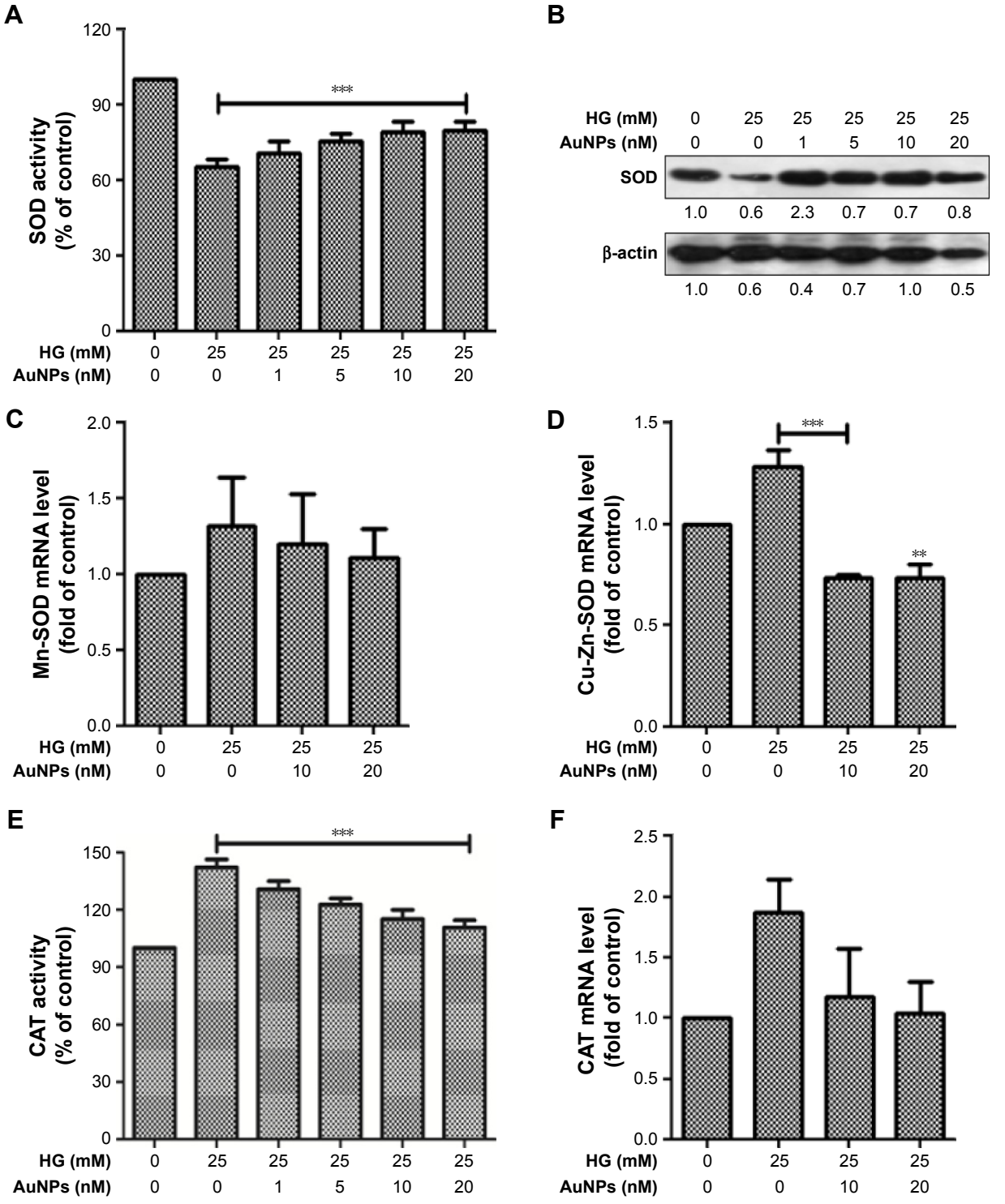

Figure 2 (*Continued*)

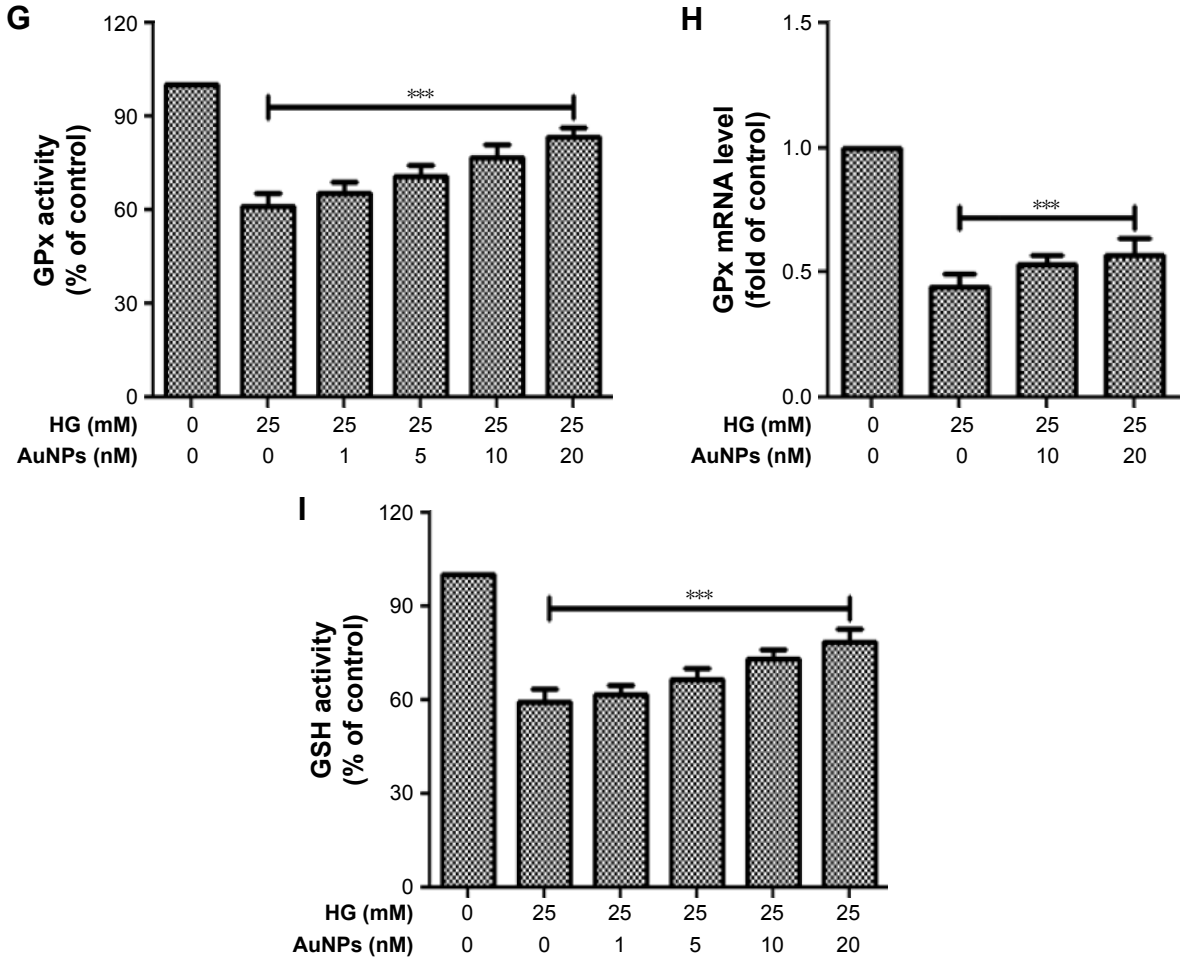

Figure 2 Effect of AuNPs on HG-induced antioxidant activities in RAW264.7 cells.
Notes: (**A**) Spectrophotometer and (**B**) immunoblot analysis of HG-induced SOD activity after exposure of AuNPs in dose-dependent manner for 24 h. qRT-PCR analysis of HG-induced (**C**) Mn-SOD and (**D**) Cu-Zn-SOD mRNA expression after exposure of AuNPs for 24 h. (**E**) Spectrophotometer and (**F**) qRT-PCR analysis of HG-induced CAT activity after exposure of AuNPs for 24 h. (**G**) Spectrophotometer and (**H**) qRT-PCR analysis of HG-induced GPx activity after exposure of AuNPs for 24 h. (**I**) Spectrophotometer analysis of HG-induced GSH activity after exposure of AuNPs in dose-dependent manner for 24 h. All experiments were performed three to four times and expressed as the mean ± standard error of the mean. $^{**}P<0.01$; $^{***}P<0.001$.
Abbreviations: AuNPs, gold nanoparticles; HG, high glucose; SOD, superoxide dismutase; qRT-PCR, quantitative real-time polymerase chain reaction; CAT, catalase; GPx, glutathione peroxidase; GSH, glutathione.

of AuNPs on HG-induced •OH production in macrophages. We observed that HG exposure increased the •OH production and dose-dependent treatment of AuNPs attenuated the •OH production in macrophages (Figure 3F and G). Similarly, AuNPs treatment attenuated the HG-induced H_2O_2 production in macrophages in a dose-dependent manner (Figure 3H and I). To check the inhibitory effect of AuNPs on HG-induced RNS production, first we studied the effect of HG on inducible nitric oxide synthase (iNOS) mRNA expression in macrophages. As shown in Figure 4A and B, the iNOS expression was up-regulated in HG-treated macrophages, whereas the expression was down-regulated after AuNPs treatment. The production of NO in HG-treated cells was significantly increased, but overproduction of NO was attenuated by AuNPs dose-dependently (Figure 4C and D). FACS analysis showed that the ONOO− accumulation in HG-exposed macrophages followed by different concentrations of AuNPs led to decrease in the number of DHR fluorescence positive cells (Figure 4E and F). For the confirmation of results obtained from the macrophages, fluorescence microscopy was also done for better understanding of the inhibitory effect of AuNPs on HG-induced ONOO− accumulation. Figure 4G showed that HG significantly increased the ONOO− production and AuNPs attenuated the ONOO− overproduction.

Inhibitory effect of AuNPs on HG-induced activation of ERK1/2MAPK/Akt, NF-κB and pro-inflammatory mediators in macrophages

The ERK1/2MAPK/Akt-mediated signaling pathway was investigated to understand the possible mechanisms involved

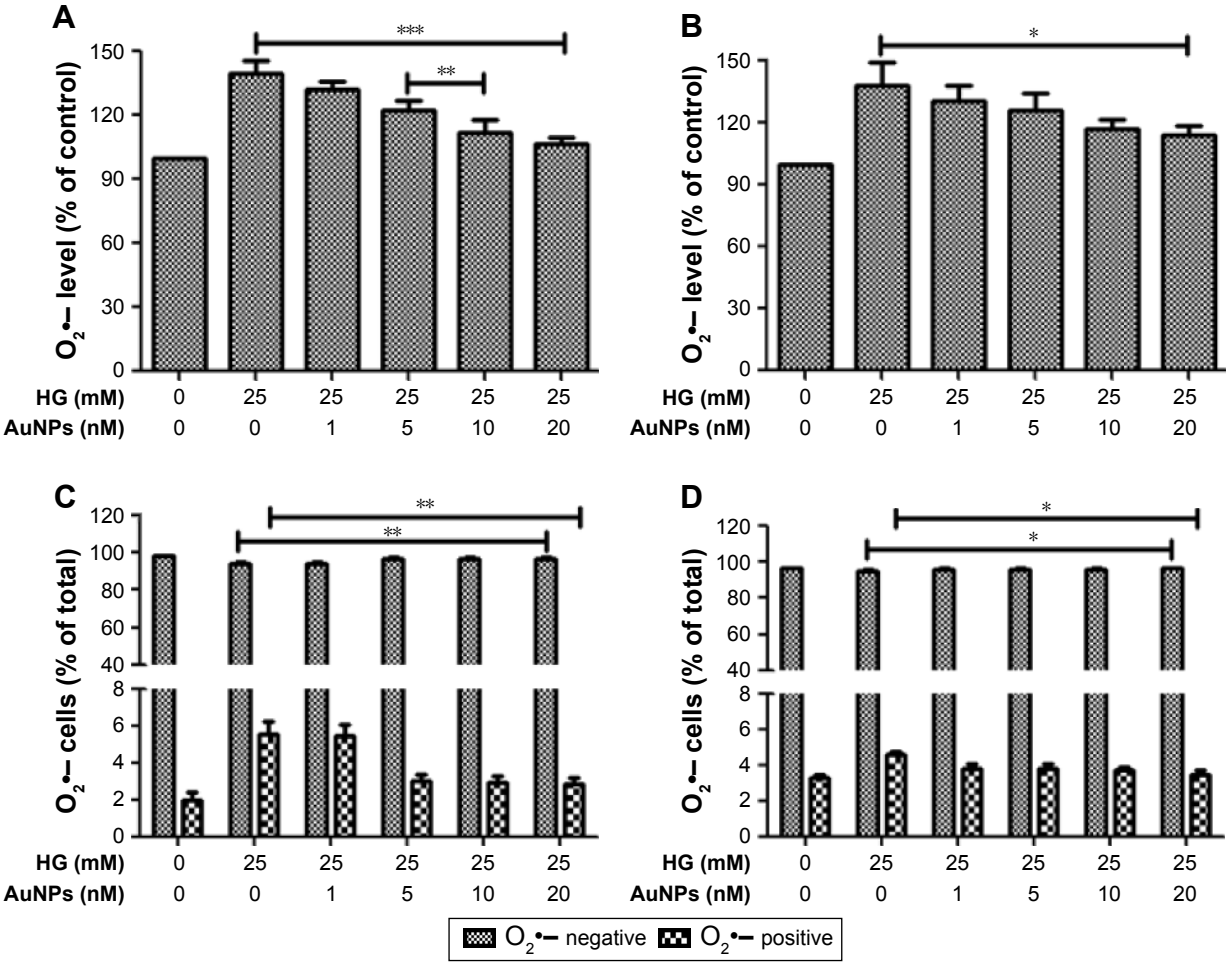

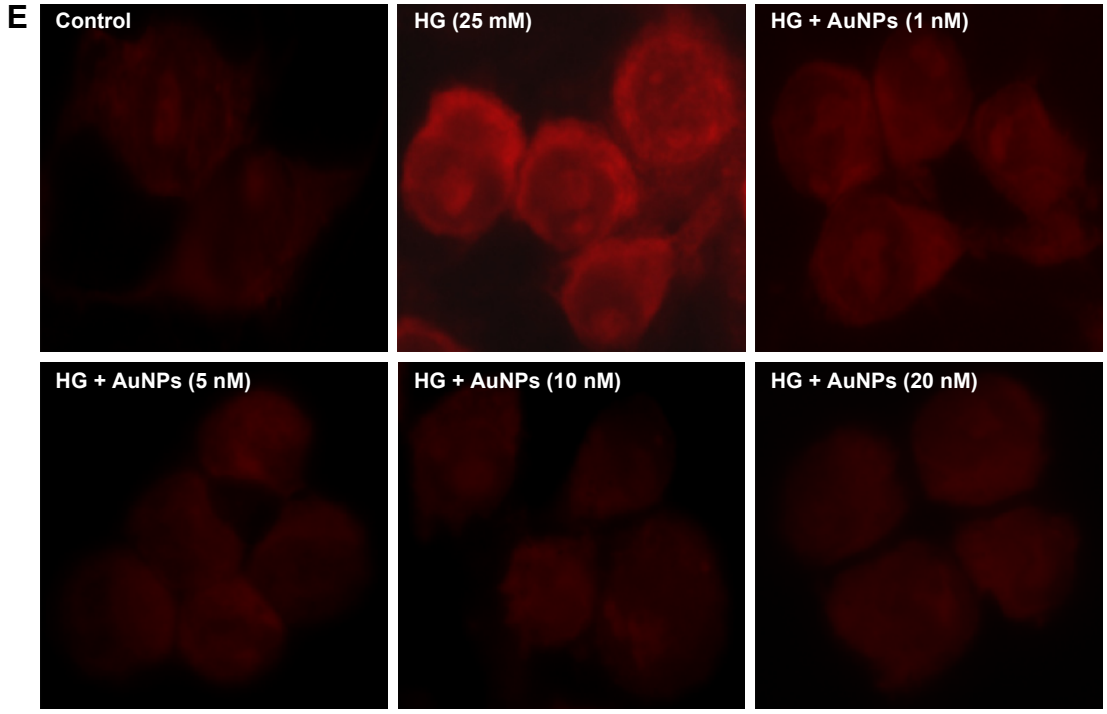

Figure 3 (*Continued*)

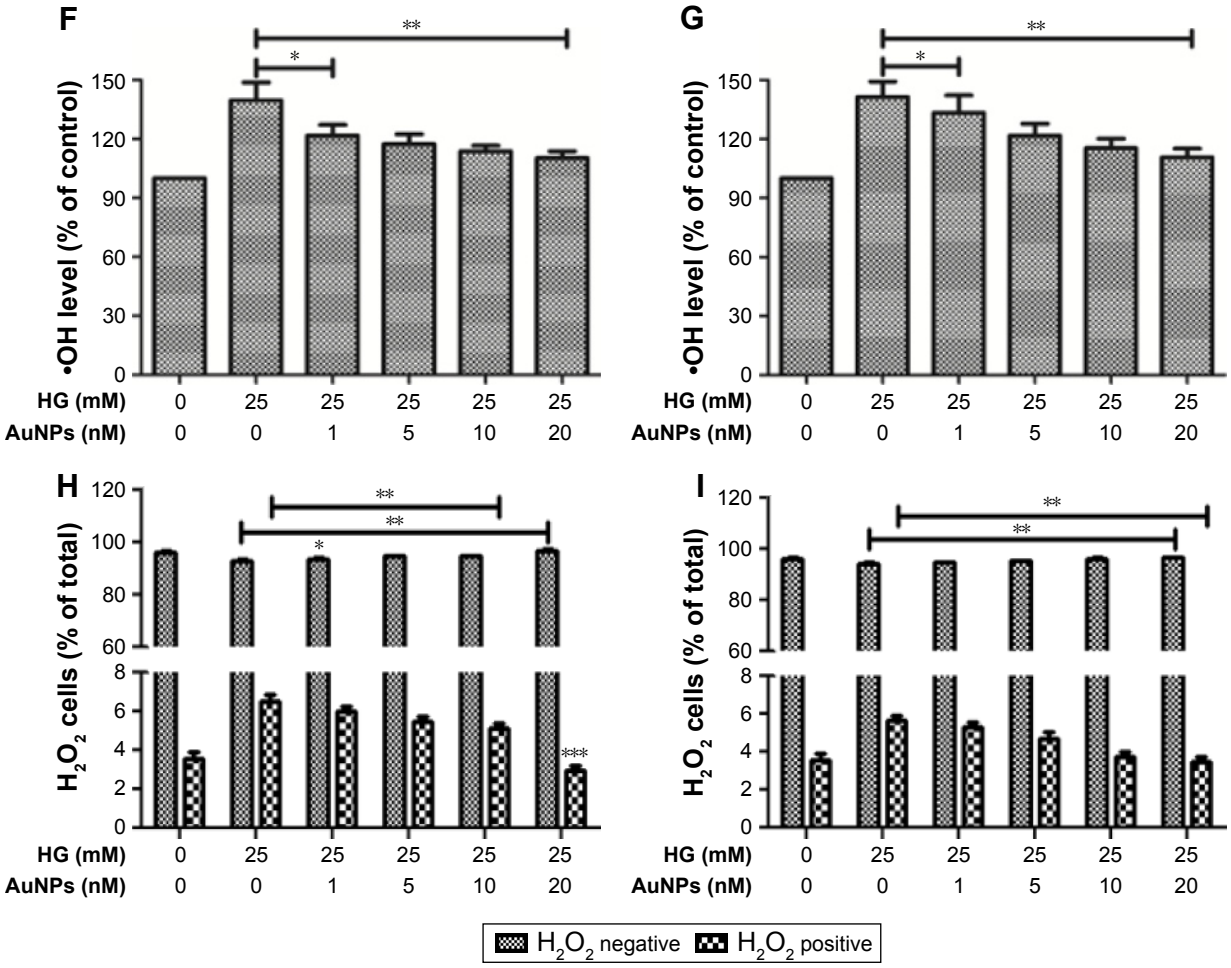

Figure 3 Effect of AuNPs on HG-induced ROS production in macrophage cells.

Notes: NBT assay shows that treatment with AuNPs attenuates $O_2^{\bullet-}$ generation in HG exposed (**A**) RAW264.7 cells and (**B**) THP-1 cells in a dose-dependent manner for 24 h. FACS analysis of $O_2^{\bullet-}$ positive cells shows a significant decrease in ROS accumulation in (**C**) RAW264.7 cells and (**D**) THP-1 cells cultured with or without HG in the presence or absence of AuNPs in a dose-dependent manner for 24 h. (**E**) Fluorescence microscopy showing decrease in $O_2^{\bullet-}$ production after exposure of AuNPs in a dose-dependent manner with or without HG for 24 h. Magnification 100×. Spectrophotometer assay of HG-induced •HO generation in (**F**) RAW264.7 and (**G**) THP-1cells after exposure of AuNPs in a dose-dependent manner for 24 h. FACS analysis of HG-induced H_2O_2 positive cells shows decrease in H_2O_2 production in (**H**) RAW264.7 cells and (**I**) THP-1 cells after AuNPs treatment. All experiments were performed three to four times and expressed as the mean ± standard error of the mean. *$P<0.05$; **$P<0.01$; ***$P<0.001$.

Abbreviations: AuNPs, gold nanoparticles; HG, high glucose; ROS, reactive oxygen species; FACS, fluorescence-activated cell sorting; NBT, nitro blue tetrazolium.

in the inhibitory effect of AuNPs on HG-induced oxidative-nitrosative stress in macrophages. We observed that HG exposure activates ERK1/2MAPK, and dose-dependent treatment of AuNPs attenuated the activation of ERK1/2MAPK in RAW264.7 cells (Figure 5A). An increase in phosphorylation of Akt/tuberin-mTOR was observed after HG exposure, but phosphorylations of Akt/tuberin-mTOR were inhibited by AuNPs dose-dependently (Figure 5B). To clarify the possible downstream oxidative-nitrosative signaling pathway involved in NF-κB activation, the effect of AuNPs on NF-κB activation in exposure to HG was investigated in the presence/absence of AuNPs in RAW264.7 cells. As shown in Figure 5C, HG exposure significantly decreased the levels of IκBα, cytoplasmic pP65 and increased level of nuclear pP65 compared with untreated one, while the AuNPs treatment restored the activity dose-dependently. To validate the inhibitory action of AuNPs, we performed immunocytochemistry assay in RAW264.7 cells. It showed that elevated expression of NF-κB in HG-treated cells was attenuated by higher doses of AuNPs (Figure 5D). To further elucidate the possible downstream oxidative-nitrosative stress-signaling pathway involved in NF-κB activation leading to induction of pro-inflammatory mediators, we measured the inhibitory effect of AuNPs after HG exposure in macrophages. Results demonstrated that mRNA expressions of cytokines (TNF-α, IL-1α), intercellular adhesion molecule (ICAM), chemokines (CXCl10, CCL8, CX3CL1), matrix metalloproteinase-2/9 (MMP-2/9) and cyclooxygenase-2 (COX-2) were

up-regulated with HG exposure, indicating HG treatment regulated a robust inflammatory response in macrophages, but the increased level of inflammation was significantly decreased by AuNPs (Figure 6A–E).

Inhibitory effect of AuNPs on HG-induced apoptosis in macrophages

We quantitatively estimated the inhibitory effect of AuNPs on HG-induced apoptosis in macrophages by MTT assay. Figure 7A and B showed that cell viability decreased significantly after exposure to HG in macrophages, and the percentage of viable cells increased after treatment with AuNPs in a dose-dependent manner. Subsequently, morphological examination was carried out by DAPI and Hoechst nuclear staining with/without treatment of AuNPs in HG condition. As shown in Figure 7C and D, S2A, HG-treated cells exhibited fragmented nuclear staining, which was attenuated in AuNPs treatment. Further, we measured the

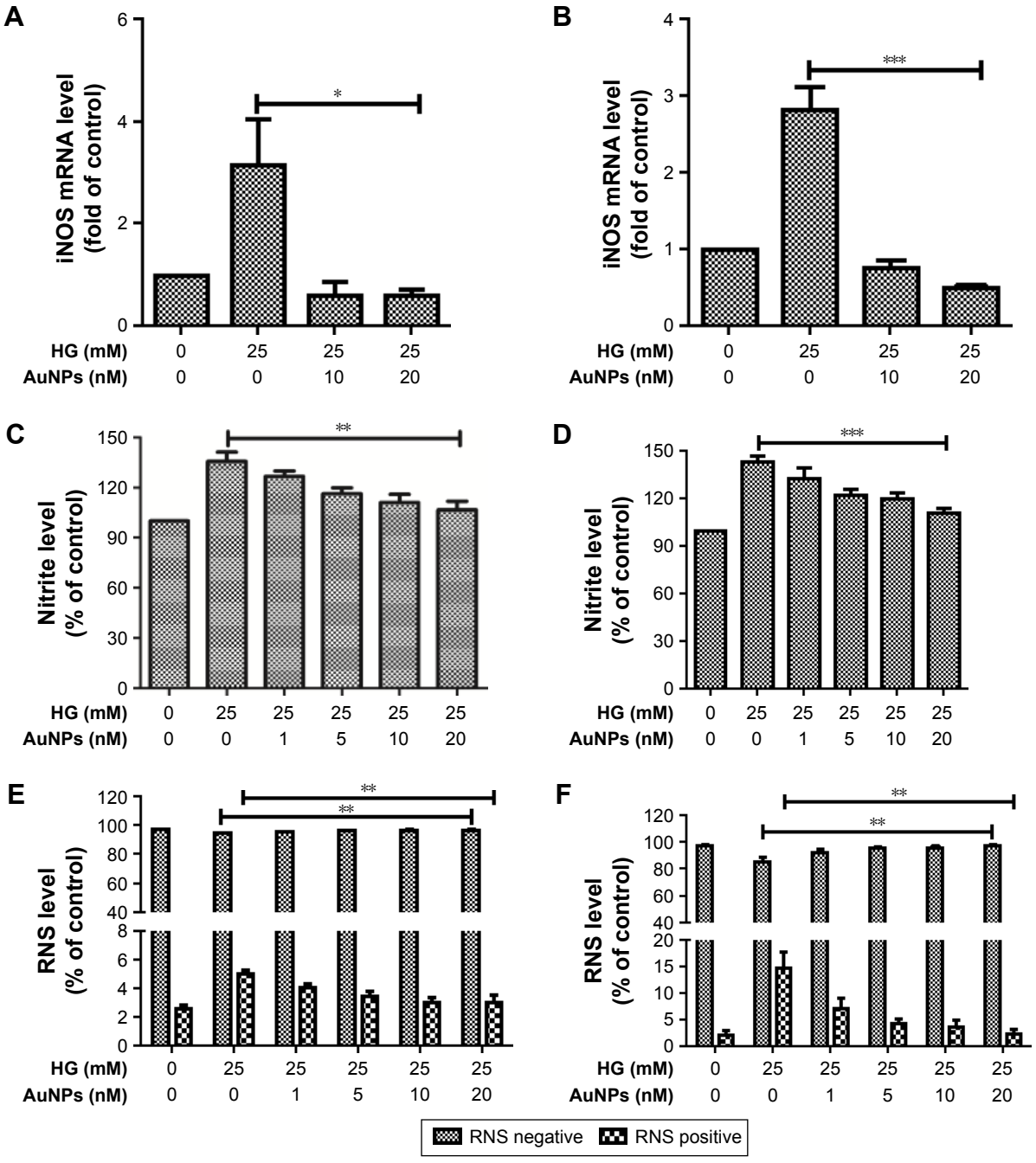

Figure 4 (*Continued*)

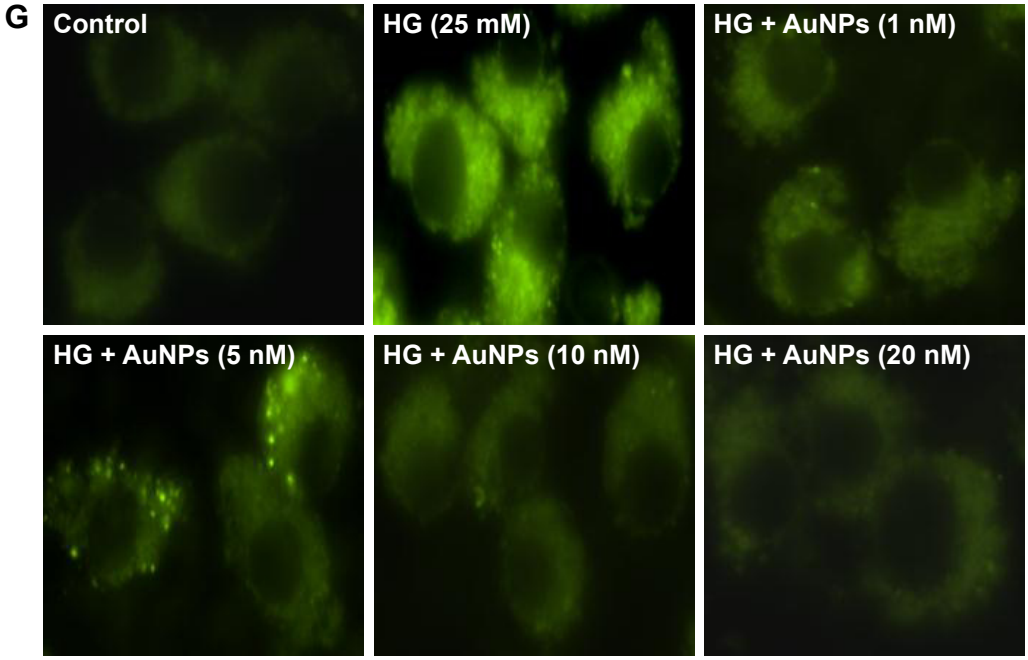

Figure 4 Effect of AuNPs on HG-induced RNS production in RAW264.7 cells.
Notes: qRT-PCR analysis of HG-induced iNOS gene expression in (**A**) RAW264.7 and (**B**) THP-1 cells after exposure of AuNPs in a dose-dependent manner for 24 h. Spectrophotometer analysis of HG-induced of NO production in (**C**) RAW264.7 and (**D**) THP-1 cells in a dose-dependent manner for 24 h. FACS analysis of $ONOO^-$ positive cells in (**E**) RAW264.7 and (**F**) THP-1 cells cultured with or without HG in the presence or absence of AuNPs in a dose-dependent manner for 24 h. (**G**) Fluorescence microscopy shows the decrease in $ONOO^-$ accumulation with treatment of AuNPs in a dose-dependent manner after exposure of HG for 24 h. Magnification 100×. All experiments were performed three to four times and expressed as the mean ± standard error of the mean. *$P<0.05$; **$P<0.01$; ***$P<0.001$.
Abbreviations: AuNPs, gold nanoparticles; HG, high glucose; qRT-PCR, quantitative real-time polymerase chain reaction; FACS, fluorescence-activated cell sorting; RNS, reactive nitrogen species.

significant activation of apoptotic markers like cytochrome c, Bax, PCNA, and caspases after HG exposure of RAW264.7 cells, which were markedly decreased after treatment with different concentrations of AuNPs (Figure 7E). However, anti-apoptotic marker Bcl-xL was decreased by HG exposure and different concentrations of AuNPs treatment for 24 h attenuated the action (Figure 7E). To evaluate the inhibitory effect of AuNPs on HG-induced cell cycle challenge, cell cycle progression was done in RAW264.7 cells. FACS analysis showed that HG exposure significantly decreased the percentage of cells in G0-phase, and increased the percentage of cells in S-phase. When cells were exposed to different concentrations of AuNPs, the percentage of cells in S-phase decreased in a dose-dependent manner (Figure 7F). Further, confirmation of cell cycle deregulation leading to apoptosis in HG condition, FITC-labeled annexin-V was carried out in macrophage cells. Figure 7G showed that a significant increase in apoptotic cells was attenuated by higher doses of AuNPs. Also, we examined the effect of AuNPs on cell cycle modulators by Western blot. As shown in Figure 7H, dose-dependent decrease of cell cycle modulators, chk1, chk2, cyclin A, cdc2 and p53, except for cyclin B1 was observed with increasing dose of AuNPs in HG-treated RAW264.7 cells. Next, we observed the changes in lysosome content by autophagosome accumulation through size-dependent AuNPs uptake and lysosome impairment in HG-treated RAW264.7 cells. Figure 7I illustrates that cells treated with HG boost more lysosomal staining – compared with control, while in cells treated with AuNPs, the staining was reduced to control level.

Inhibitory effect of AuNPs on HG-induced biomolecules damage in macrophages

HG treatment immensely affects the LPO and PC in macrophages. The LPO and PC levels were significantly decreased after exposure to AuNPs in a dose-dependent manner in HG-treated macrophages (Figure 8A and B). Further, we checked the DNA damage in cells treated with HG followed by treatment with AuNPs for 24 h. During the single cell gel electrophoresis assay, it was observed that DNA migrated more rapidly toward the anode in HG-treated cells and cells treated with AuNPs attenuated the DNA migration (Figure 8C). To further confirm that DNA damage in HG exposure was attenuated by AuNPs, we performed DNA ladder assay in macrophage cells. Figure 8D showed that most DNA fragmentation was observed in cells exposed to HG, and DNA

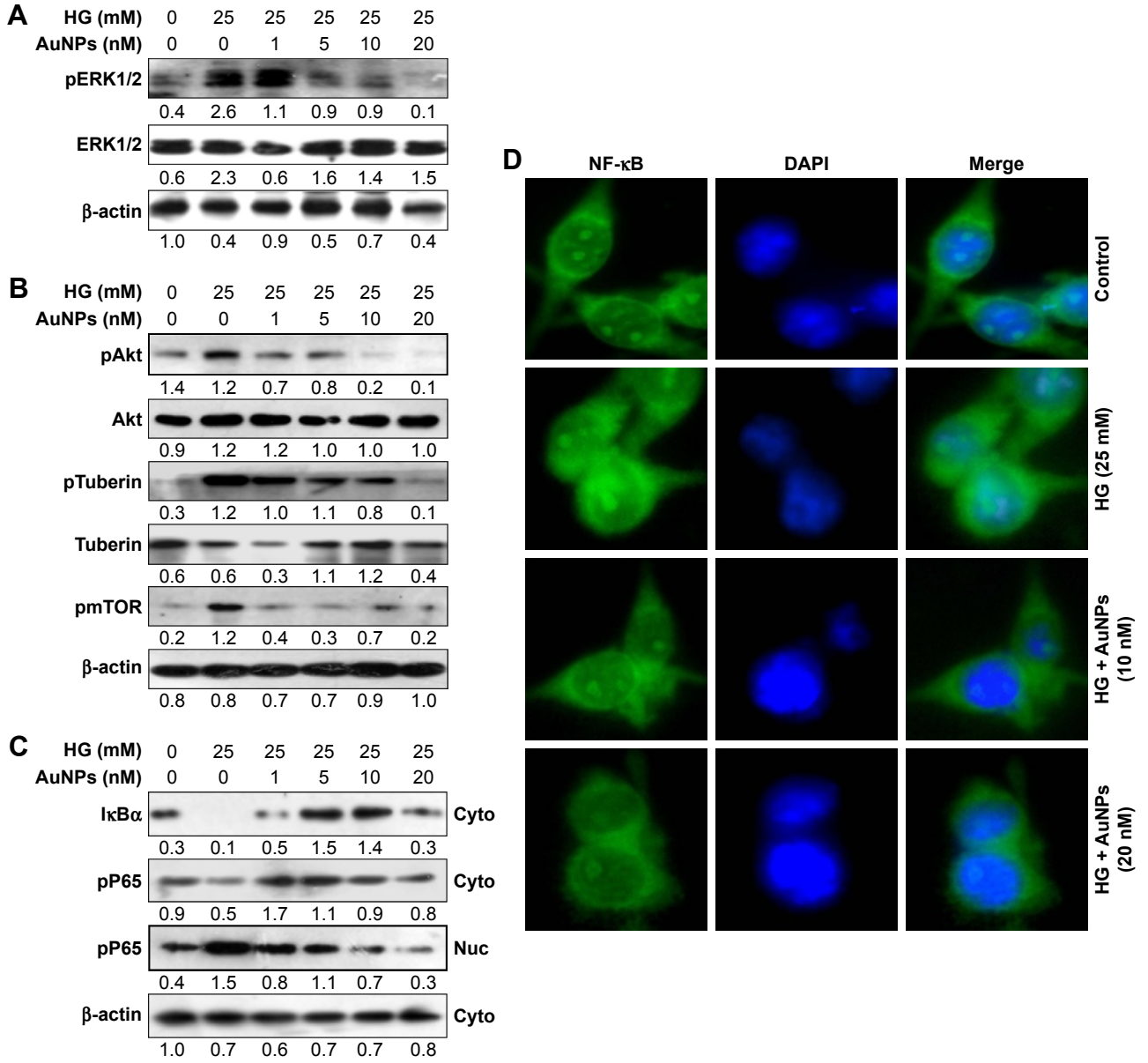

Figure 5 Effect of AuNPs on HG-induced signaling cascades in RAW264.7 cells.

Notes: A representative immunoblot of RAW264.7 cells exposed to HG with different concentrations of AuNPs shows an increase in phosphorylation of (**A**) ERK1/2MAPK and (**B**) Akt, tuberin and mTOR after 24 h. (**C**) After HG treatment, a significant decrease in the levels of IκBα, cytoplasmic pP65 and an increase in level of nuclear pP65 was observed that was restored after treatment with AuNPs in a dose-dependent manner for 24 h. (**D**) A representative immunocytochemistry analysis shows the NF-κB activation in HG exposure and downregulation after treatment with AuNPs in RAW264.7 cells for 24 h. Magnification 100×.

Abbreviations: AuNPs, gold nanoparticles; HG, high glucose; MAPK, mitogen-activated protein kinase; mTOR, mammalian target of rapamycin; NF-κB, nuclear factor κB; Cyto, cytoplasmic; Nuc, nucleoplasmic.

fragmentation was attenuated when cells were treated with AuNPs. Next, we established that DNA damage was attenuated by AuNPs in HG-treated RAW264.7 cells by Western blotting. Figure 8E shows the decrease of pATM, pATR and pH2A.X with increasing dose of AuNPs in HG-treated cells. OGG1 is a DNA repair marker that excises 8-OHdG. As shown in Figure 8F, the protein expression of OGG1 in HG-treated RAW264.7 cells was less in comparison with untreated control, but AuNPs treatment leads to the increase in protein expression after 24 h. For further confirmation, we performed qRT-PCR assay and observed that after HG exposure, mRNA expression of OGG1 was decreased and treatment with AuNPs, mRNA level of OGG1 was increased in macrophages (Figure 8G). Additionally, to validate the OGG1 attenuation by AuNPs after HG exposure, we performed immunofluorescence assay. Figure 8H showed that expression of OGG1 after HG exposure improved in AuNPs treated RAW264.7 cells. Next, we measured the 8-OHdG level in HG-treated RAW264.7 cells after treatment with AuNPs. As shown in Figure 8I, HG exposure significantly

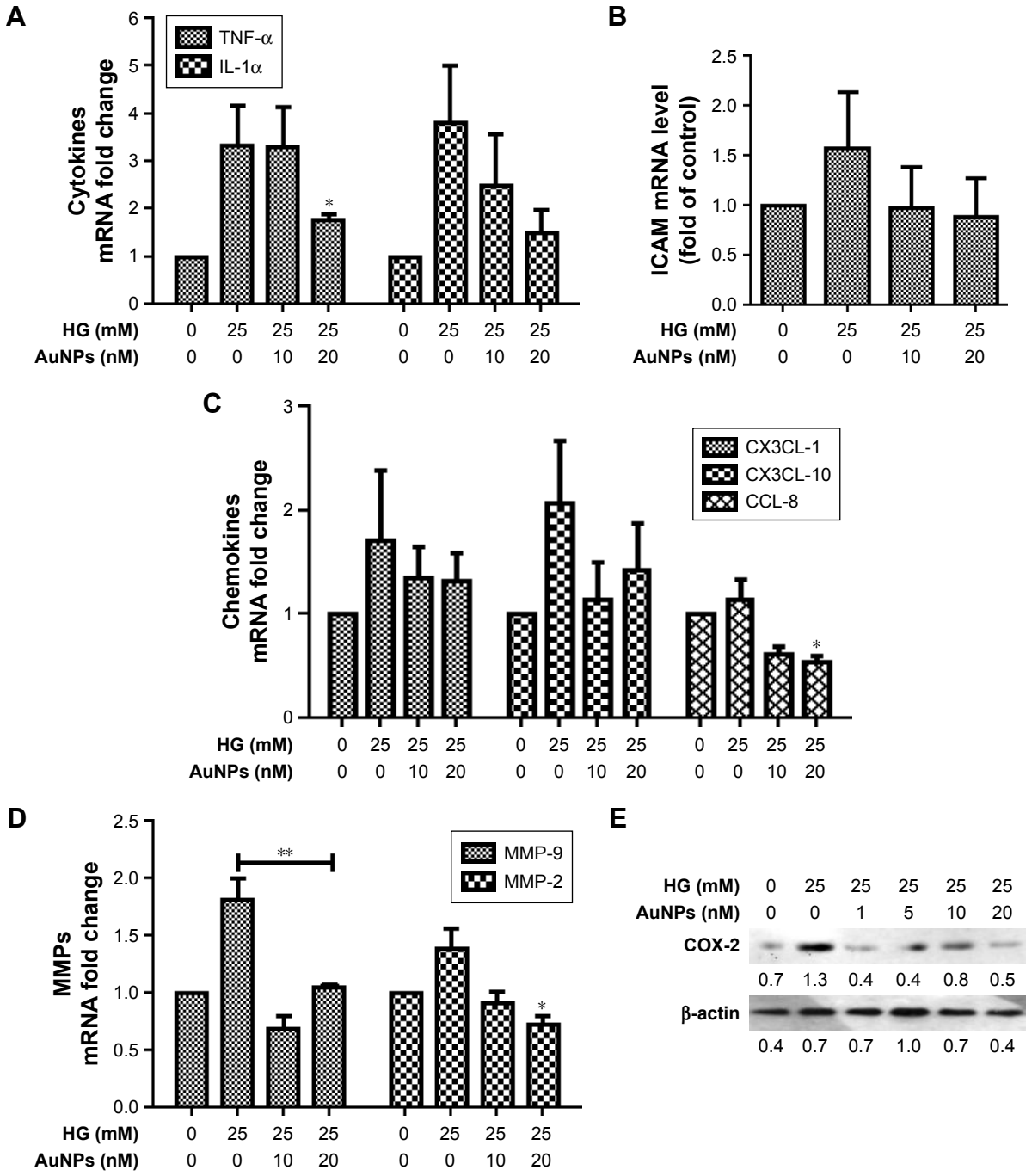

Figure 6 Effect of AuNPs on HG-induced expression of pro-inflammatory mediators in RAW264.7 cells.

Notes: qRT-PCR analysis of (**A**) TNF-α, IL-1α, (**B**) ICAM, (**C**) CX3CL-10, CCL-8, CX3CL-1, (**D**) MMP-2/-9 shows a significant increase in expression after HG exposure in RAW264.7 cells; however, treatment with AuNPs decreased the expression of all the above genes in a dose-dependent manner after 24 h. (**E**) A representative immunoblot of RAW264.7 cells exposed to HG with different concentrations of AuNPs shows an increase in COX-2 protein expression after 24 h. *$P<0.05$; **$P<0.01$.

Abbreviations: AuNPs, gold nanoparticles; HG, high glucose; COX, cyclooxygenase; TNF, tumor necrosis factor; IL, interleukin; qRT-PCR, quantitative real-time polymerase chain reaction; MMP, matrix metalloproteinase.

increased the levels of 8-OHdG in comparison with untreated one, while pretreatment of AuNPs restored the activity.

Discussion

Atherosclerosis, a chronic inflammatory disease, is initiated by the activation of endothelial cells following excess accumulated adhesion of activated and foamed monocytes/macrophages in the intima.[26,27] More importantly, foamed macrophages generate ROS/RNS, and secrete inflammatory mediators, leading to neointima hypertrophy and infarction.[28,29] Our previous findings demonstrated that cellular signaling pathways mediated by ROS/RNS in cellular compartments

were associated with each other by elevated glucose in macrophages activation leading to apoptosis and inflammation, and these processes exacerbated atherogenesis.[2] Therefore, scavenging the excess production of ROS/RNS due to HG exposure regulates monocyte/macrophage adhesion to endothelial cells as well as blockade of foaming cell formation may restrain the progression of atherosclerosis. Accumulating evidence indicates that AuNPs have received great

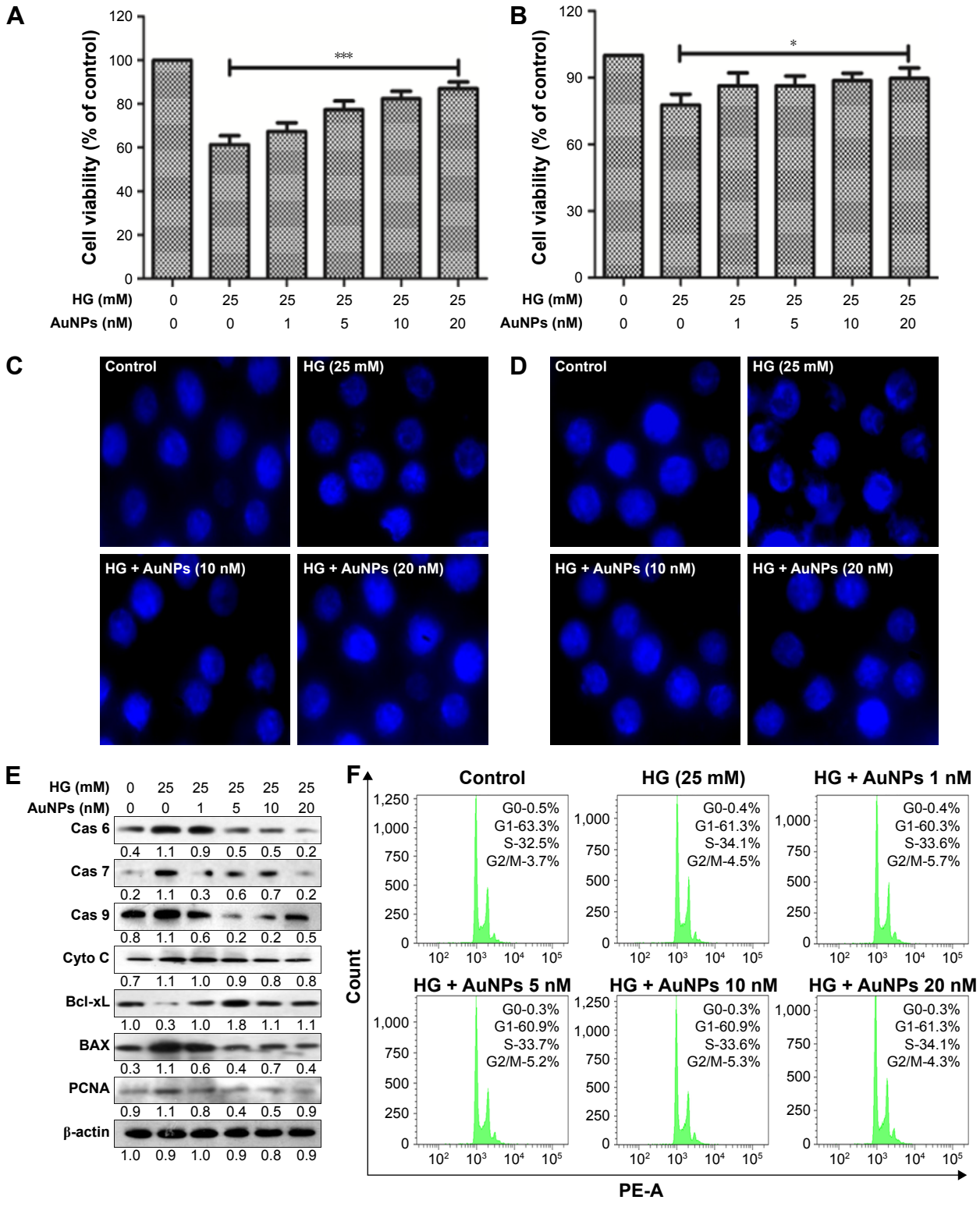

Figure 7 (*Continued*)

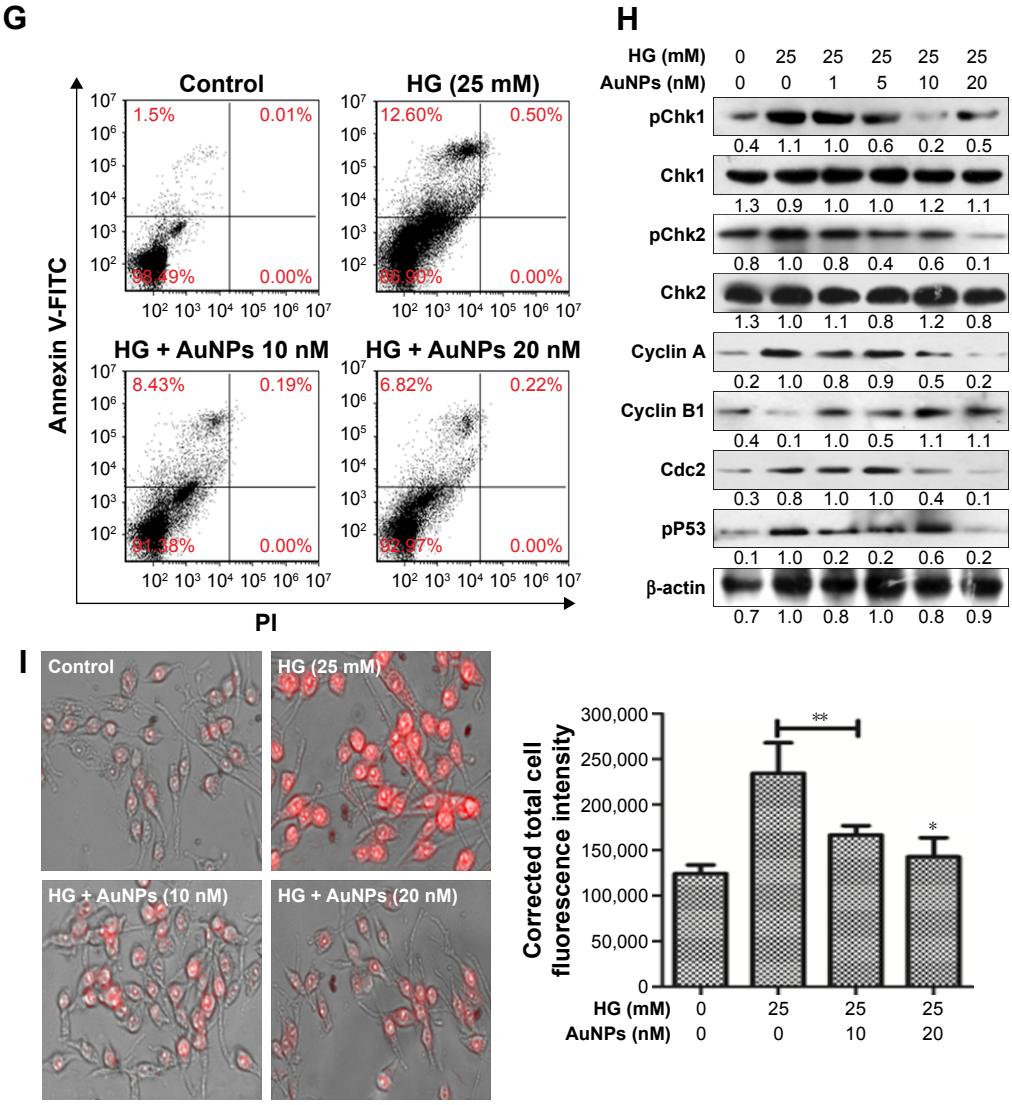

Figure 7 Effect of AuNPs on HG-induced apoptosis in macrophage cells.

Notes: MTT assay shows the cell viability decreases in HG-induced (**A**) RAW264.7 cells and (**B**) THP-1 cells, but cell viability increases after exposure with increasing concentrations of AuNPs for 24 h. DAPI staining shows the apoptotic cells in their appearance as shrunken, irregular or fragmented nuclei in HG-exposed (**C**) RAW264.7 cells and (**D**) THP-1 cells, and restored normal shape in AuNPs treatment for 24 h. (**C**) Magnification 40×. (**E**) A representative immunoblot analysis of apoptotic markers such as cytochrome c, Bcl-xL, BAX, PCNA caspase-6, caspase-7 and caspase-9 in the presence or absence of AuNPs after HG-exposure for 24 h. (**F**) A representative FACS analysis shows the percentage of G0-phase significantly decreased, whereas G1-phase increased after AuNPs treatment after exposure to HG for 24 h. (**G**) FACS analysis shows increasing numbers of apoptotic cells in HG-cultured RAW264.7 cells, while treatment with AuNPs decreased the number of apoptotic cells in a dose-dependent manner after 24 h. (**H**) A representative immunoblot analysis shows the cell cycle regulating molecules such as Chk1, Chk2, Cdc2, cyclin A, cyclin B1 and pP53 in the presence or absence of AuNPs after HG exposure for 24 h. (**I**) Fluorescence microscopy analysis shows increase in lysosomal activity in HG condition, but activity is decreased with AuNPs treatment in RAW264.7 cells after 24 h. Magnification 20×. All the experiments were performed three to four times and expressed as the mean ± standard error of the mean. *$P<0.05$; **$P<0.01$; ***$P<0.001$.

Abbreviations: AuNPs, gold nanoparticles; HG, high glucose; PCNA, proliferating cell nuclear antigen; FACS, fluorescence-activated cell sorting; PI, propidium iodide; FITC, fluorescein isothiocyanate.

attention as an emerging nanomedicine and are renowned for their promising therapeutic possibilities, due to their biocompatibility, high surface reactivity, and resistance to oxidation.[30,31] The inhibitory activity of AuNPs against inflammatory mediators-induced increase in endothelial cell numbers provides clear evidence of their therapeutic potential in the treatment of different inflammatory-related complications.[32]

Previous studies showed that AuNPs did not show any cytotoxic effect when taken up by cells.[33,34] In the present study, the fractions of enriched serum proteins were observed when cell culture medium for macrophage cells was concentrated and subjected to protein corona analysis. Fortunately, we did not observe any AuNPs tendency to agglomerate in the cell culture medium that will cause toxicity to macrophages. Subsequently, by using MTT assay, the

nontoxic nature of AuNPs alone was confirmed (Figure S1) and observed that 1–20 nM doses were not showing any toxic effect to macrophages, but after 20 nM, it became toxic to the cells. Therefore, following confirmation of the nontoxic nature of AuNPs, HG-induced oxidative-nitrosative stress regulated biomolecules damage and apoptosis via NF-κB/ERK1/2/Akt pathways in macrophages were investigated. Studies have demonstrated that augmented glucose flux

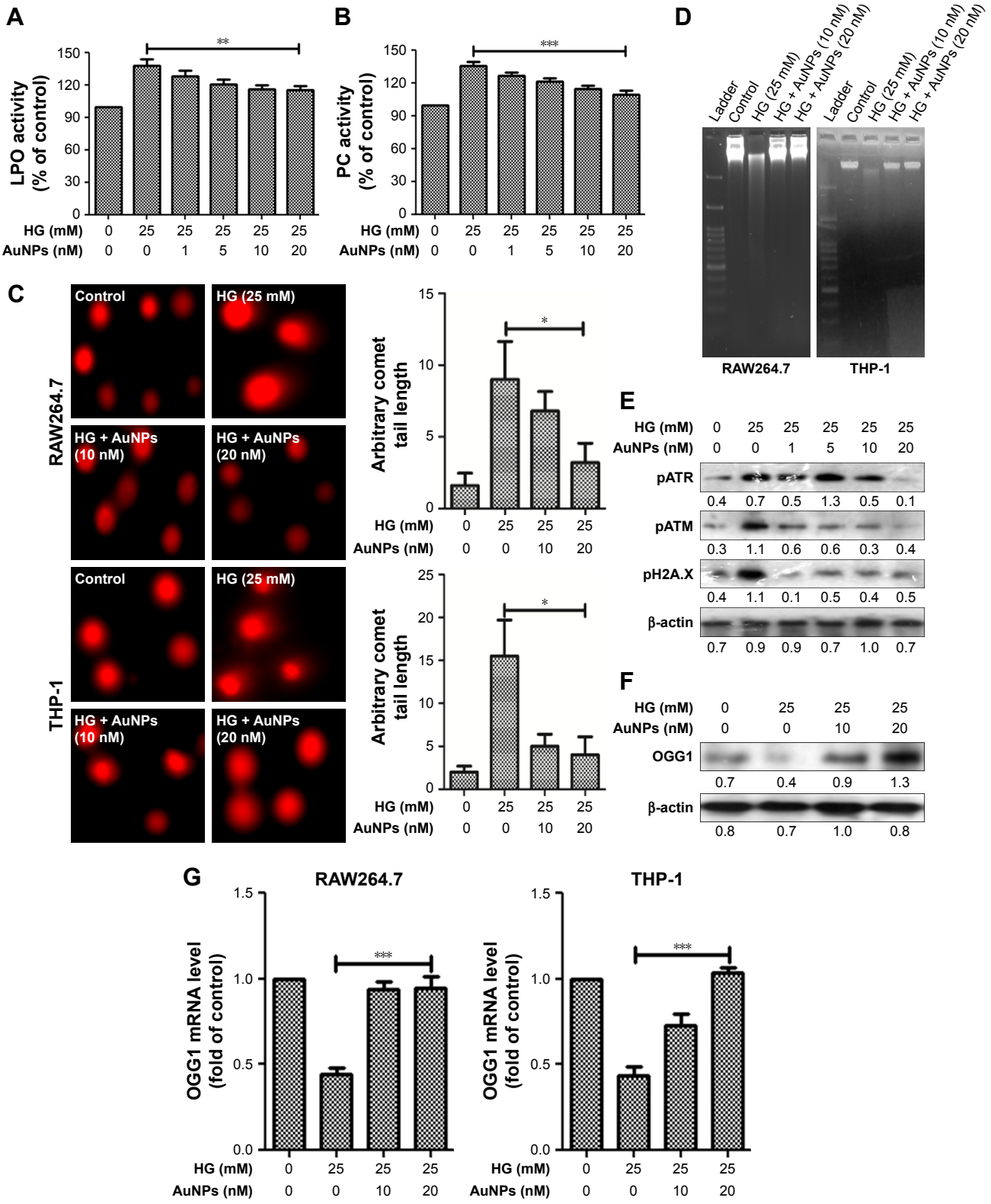

Figure 8 (*Continued*)

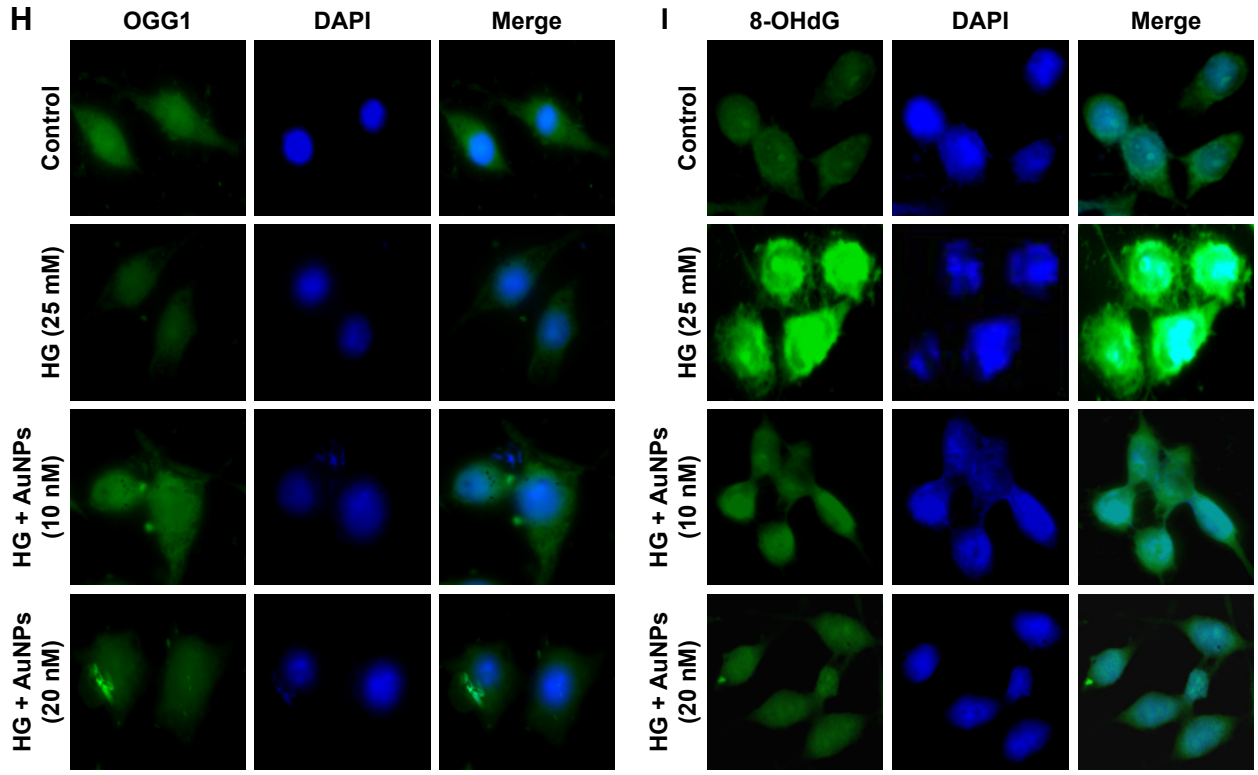

Figure 8 Effect of AuNPs on HG-induced biomolecules damage in macrophages.

Notes: Spectrophotometer analysis of HG-induced (**A**) LPO and (**B**) PC level after exposure of AuNPs in a dose-dependent manner for 24 h. (**C**) A representative comet assay shows the HG-induced DNA damage in RAW264.7 and THP-1 cells, while treatment with AuNPs for 24 h induced recovery of the DNA damage in both the cells. Magnification 100×. (**D**) Agarose gel electrophoresis analysis shows the DNA fragmentation after exposure to HG, while treatment with AuNPs for 24 h, restored the DNA fragmentation in RAW264.7 and THP-1 cells. (**E**) A representative immunoblot analysis of DNA damage markers, ATR, ATM and H2A.X shows phosphorylation in HG exposure, which is attenuated after AuNPs treatment for 24 h. (**F**) A representative immunoblot of OGG1 protein expression in HG-induced RAW264.7 cells, which is attenuated after exposure to AuNPs for 24 h. (**G**) qRT-PCR analysis of *OGG1* gene in RAW264.7 and THP-1 cells in the presence or absence of AuNPs after HG-exposure for 24 h. A representative immunocytochemistry analysis of (**H**) OGG1 and (**I**) 8-OHdG in the presence or absence of AuNPs after HG-exposure for 24 h. Magnification 100×. All experiments were performed three to four times and expressed as the mean ± standard error of the mean. $^{*}P<0.05$; $^{**}P<0.01$; $^{***}P<0.001$.

Abbreviations: AuNPs, gold nanoparticles; HG, high glucose; LPO, lipid peroxidation; PC, protein carbonylation; qRT-PCR, quantitative real-time polymerase chain reaction.

enhances the intracellular oxidants and impairs antioxidant defenses by multiple signaling pathways.[3,35] More importantly, cells contain a large number of antioxidants to prevent or repair the damage caused by ROS/RNS, as well as regulate redox-sensitive signaling cascades in diverse cell types during hyperglycemia.[4,36] The SOD neutralizes $O_2^{\bullet-}$ into H_2O_2 and O_2, while the CAT detoxifies the H_2O_2 to nontoxic H_2O.[37] Similarly, the GPx reduces organic hydroperoxides, while GSH helps in the redox regulation of cellular compartments and offers a defense mechanism against oxidant stress in a thiol-sensitive fashion.[38] Our results show that the activity of antioxidants such as SOD, GPx and GSH decreases in HG condition in macrophages, but the antioxidants level improved with increasing dose of AuNPs. Further, at mRNA level, the expression of Mn-SOD/Cu-Zn-SOD was higher in HG condition, but AuNPs attenuated the elevated mRNA expression, which coincided with the findings of others.[39] Interestingly, CAT activity was elevated with HG in RAW264.7 cells and the expression was attenuated by AuNPs. Our results show that the AuNPs potential as an antioxidant was shored up with glucose flux in macrophages and the findings correlated with previous reports delivering the control effects of AuNPs as an antioxidant.[40] Furthermore, overproduction of ROS/RNS after HG exposure that led to the oxidative-nitrosative stress was attenuated by different concentration of AuNPs. Ten to twenty nanomolar doses of AuNPs showed a significant decrease in the level of ROS/RNS somewhat similar to the control compared with HG. Elevated level of NO and ONOO– in HG-treated cells led to nitrosative stress, and potential protective effects of AuNPs control the overproduction of NO and ONOO−. Thus, these findings confirm the potential role of AuNPs in eliminating the ROS/RNS after HG exposure, thereby restoring the balanced level of antioxidants defense mechanisms, and support the therapeutic potential of AuNPs as a promising antioxidant.

Studies have indicated that HG-induced oxidative-nitrosative stress induces the activation of ERK1/2MAPK/Akt signaling pathways.[4] Our recent publications and other

studies also suggested that water-soluble antioxidants suppressed the glucose-induced ERK1/2MAPK/Akt activation in different cell types, including macrophages, and involved oxidative-nitrosative stress regulates signaling cascades as intermediate molecules, transducing signals from ERK1/2MAPK/Akt to NF-κB.[4,41] In accordance with our current results, we found that AuNPs block glucose-induced NF-κB activation, thus identifying these transcriptional factors as downstream signaling of ROS/RNS and targets through ERK1/2MAPK/Akt/tuberin-mTOR kinases. Taken together, these results indicated that increased production of intracellular ROS/RNS and activation of ERK1/2MAPK/Akt/tuberin-mTOR pathways were initial signaling events in the regulation of *NF-κB* gene by HG, and all these activities were restored by AuNPs. Recently, AuNPs have received great interest as anti-inflammatory agents through their ability to inhibit expression of NF-κB and subsequent inactivation of inflammatory mediators in diverse cell types. Our results are also supported by the findings that the non-cytotoxic effect of AuNPs, and their knack to reduce the production of ROS/RNS, which does not elicit secretion of pro-inflammatory mediators, including cytokines (TNF-α, IL-1α), chemokines (CX3CL1, CXCL10, CCL8), ICAM, MMP-2/-9, and COX-2 makes them a suitable candidate for nanomedicine. Therefore, inhibition of oxidative-nitrosative stress leading to NF-κB inactivation via ERK1/2MAPK/Akt/tuberin-mTOR kinases is thought to be a molecular target for therapeutic intervention in HG-induced transcriptionally regulated inflammation in macrophages.

The ROS/RNS are highly oxidative/nitrosative molecules, which function as physiological regulators of intracellular signal pathways as well as cytotoxic in diverse cell types, and they induce cell death, either by apoptosis or by necrosis through oxidation.[2–4] Our prior studies showed that under hyperglycemic condition, mitochondria released apoptosis-inducing factors that may trigger nuclear DNA fragmentation.[4] In contrast, our current results showed that when macrophage cells were exposed to HG, the number of live cells was significantly decreased, and increased the viable cells population when cells were exposed to various concentrations of AuNPs. Furthermore, the DNA fragmentation and general morphological analysis of nuclei confirmed the protective effect of AuNPs and showed that apoptotic cell death in HG-exposed cells was decreased. The cells were arrested at S-phase of cell cycle because of DNA damage. We observed that elevated expression of chk1, chk2, cdc2, cyclin A, cyclin B1 and p53 in HG exposed macrophages deceased after treatment with AuNPs. Similarly, under HG condition, the level of apoptotic markers like caspases, cytochrome C, Bax, and PCNA was elevated and the expression of anti-apoptotic markers like Bcl.xL protein level decreased, leading to the apoptosis, which was inhibited by AuNPs. More importantly, to confirm the caspases, Bax and Bcl.xL9 expression was reduced more than in control, an indication of the apoptotic effects of AuNP, which we validated by including an AuNP only control group (Figure S2B). Moreover, recent studies have demonstrated that autophagy was most active in the G1 and S phases of the cell cycle,[42] which were linked between autophagy induction and increased in the proliferation rate.[43,44] Additionally, Matus et al[45] revealed in his reports that autophagy was a major protective mechanism underlying oxidative stress to overcome some degenerative diseases. In our present study, we also assessed the lysomal activity in macrophage cells treated with AuNPs in the presence/ absence of HG and our data coincided with the above findings.

Studies have revealed that PI3-K/ERK1/2MAPK/Akt/tuberin/OGG1 pathway was relevant in HG exposure and may contribute to oxidative-nitrosative stress-stimulated macrophages activation.[2] Also, we observed that PI3-K/Akt and ERK1/2MAPK inhibitors blocked the effect of HG on tuberin-mTOR activation, indicating that PI3-K/ERK1/2MAPK/Akt pathways were mediated by the action of HG on tuberin-mTOR in macrophages.[2] Furthermore, tuberin-mTOR activity has been positively correlated with the level of OGG1 in diabetic condition.[4,46] Here, our results demonstrated that HG-induced tuberin-mTOR phosphorylation by ERK1/2MAPK/Akt had biological consequences; like a decrease in OGG1 expression in macrophage cells was attenuated by AuNPs. The 8-OHdG is known to be a sensitive DNA damage marker and accumulated in DNA after oxidative-nitrosative stress.[4] Interestingly, the accumulated 8-OHdG in DNA was removed by specific enzymatic cleavages actively when generated after the ROS/RNS-induced 8-hydroxylation of guanine bases takes place in cellular compartments.[4,47] Mariappan et al[48] demonstrated that 8-OHdG appears to play a critical role in cell injury via the induction of apoptotic cell death, and we also recorded similar results in macrophages during HG insults and restored by AuNPs.

Conclusion

Our results suggested that AuNPs may modulate antioxidant defense mechanisms, oxidative-nitrosative free radicals scavenging, DNA damage response, enhanced macrophages proliferation, and anti-inflammatory agents. These effects may be termed hermetic due to the fact that AuNPs treatment reduces the activation of NF-κB by ERK1/2MAPK/Akt/tuberin-mTOR

pathways-mediated targeted inflammatory genes expression and cellular stress responses, resulting in the improved maintenance, repair and function of macrophages, which may be beneficial for minimizing the macrophages activation and foam cell formation in the arterial region of the blood vascular system due to HG. As human exposure to diverse nanomaterials is rapidly increasing in different pathophysiological conditions, it seems valuable to study in detail the subsequent physiological effects of AuNP-mediated cardiovascular changes, including atherosclerosis that occurs in diabetes in animal models.

Acknowledgments

The authors gratefully acknowledge funding from the Department of Biotechnology, government of India (BT/PR14241/MED/30/423/2010) to Dr Arttatrana Pal. They also thank Department of Sciences and Technology, government of India (SB/FT/CS/-096/2012) for the Ramanujan Fellowship to Satyabrata Si and University Grant Commission-Maulana Azad National Fellowship to Huma Rizwan.

Disclosure

The authors report no conflicts of interest in this work.

References

1. Bornfeldt KE. Does elevated glucose promote atherosclerosis? Pros and Cons. *Circ Res*. 2016;119(2):190–193.
2. Kumar P, Swain MM, Pal A. Hyperglycemia-induced inflammation caused down-regulation of 8-oxoG-DNA glycosylase levels in murine acrophages is mediated by oxidative-nitrosative stress-dependent pathways. *Int J Biochem Cell Biol*. 2016;73:82–98.
3. Xie L, Gu Y, Wen M, et al. Hydrogen sulfide induces Keap1 S-sulfhydration and suppresses diabetes-accelerated atherosclerosis via Nrf2 activation. *Diabetes*. 2016;65(10):3171–3184.
4. Kumar P, Raman T, Swain MM, Mishra R, Pal A. Hyperglycemia-induced oxidative-nitrosative stress induces inflammation and neurodegeneration via augmented tuberous sclerosis complex-2 (TSC-2) activation in neuronal cells. *Mol Neurobiol*. 2017;54(1):238–254.
5. Giugliano D, Ceriello A, Paolisso G. Oxidative stress and diabetic vascular complications. *Diabetes Care*. 1996;19(3):257–267.
6. Xu W, Liu LZ, Loizidou M, Ahmed M, Charles IG. The role of nitric oxide in cancer. *Cell Res*. 2002;12(5–6):311–320.
7. Tolins JP, Shultz PJ, Raij L. Role of endothelium-derived relaxing factor in regulation of vascular tone and remodeling. Update on humoral regulation of vascular tone. *Hypertension*. 1991;17(6 Pt 2):909–916.
8. Pacher P, Beckman JS, Liaudet L. Nitric oxide and peroxynitrite in health and disease. *Physiol Rev*. 2007;87(1):315–424.
9. Ceriello A. The possible role of postprandial hyperglycaemia in the pathogenesis of diabetic complications. *Diabetologia*. 2003;46:M9–M16.
10. Maiese K, Morhan SD, Chong ZZ. Oxidative stress biology and cell injury during type 1 and type 2 diabetes mellitus. *Curr Neurovasc Res*. 2007;4(1):63–71.
11. Kumar P, Rao GN, Pal BB, Pal A. Hyperglycemia-induced oxidative stress induces apoptosis by inhibiting PI3-kinase/Akt and ERK1/2 MAPK mediated signaling pathway causing downregulation of 8-oxoG-DNA glycosylase levels in glial cells. *Int J Biochem Cell Biol*. 2014;53:302–319.
12. Ferenbach D, Kluth DC, Hughes J. Inflammatory cells in renal injury and repair. *Semin Nephrol*. 2007;27(3):250–259.
13. Jin R, Zeng C, Zhou M, Chen Y. Atomically precise colloidal metal nanoclusters and nanoparticles: fundamentals and opportunities. *Chem Rev*. 2016;116(18):10346–10413.
14. Si S, Pal A, Mohanta J, Satapathy S. Gold nanostructure materials in diabetes management. *J Phys D*. 2017;50(13):134003.
15. Schiener M, Hossann M, Viola JR, et al. Nanomedicine-based strategies for treatment of atherosclerosis. *Trends Mol Med*. 2014;20(5):271–281.
16. Turkevich J, Stevenson PC, Hillier J. A study of the nucleation and growth processes in the synthesis of colloidal gold. *Discuss Faraday Soc*. 1951;11:55–75.
17. Mytych J, Zebrowski J, Lewinska A, Wnuk M. prolonged effects of silver nanoparticles on p53/p21 pathway-mediated proliferation, DNA damage response, and methylation parameters in HT22 hippocampal neuronal cells. *Mol Neurobiol*. 2017;54(2):1285–1300.
18. Weydert CJ, Cullen JJ. Measurement of superoxide dismutase, catalase and glutathione peroxidase in cultured cells and tissue. *Nat Protoc*. 2010;5(1):51–66.
19. Kapoor R, Kakkar P. Protective role of morin, a flavonoid, against high glucose induced oxidative stress mediated apoptosis in primary rat hepatocytes. *PLoS One*. 2012;7(8):e41663.
20. Subramanian MV, James TJ. Age-related protective effect of deprenyl on changes in the levels of diagnostic marker enzymes and antioxidant defense enzymes activities in cerebellar tissue in Wistar rats. *Cell Stress Chaperones*. 2010;15(5):743–751.
21. Manikandan R, Thiagarajan R, Beulaja S, Sudhandiran G, Arumugam M. Curcumin prevents free radical-mediated cataractogenesis through modulations in lens calcium. *Free Radic Biol Med*. 2010;48(4):483–492.
22. Wang Q, Zheng XL, Yang L, et al. Reactive oxygen species-mediated apoptosis contributes to chemosensitization effect of saikosaponins on cisplatin-induced cytotoxicity in cancer cells. *J Exp Clin Cancer Res*. 2010;29(1):159.
23. Sagar S, Parida SR, Sabnam S, et al. Increasing NO level regulates apoptosis and inflammation in macrophages after 2-chloroethyl ethyl sulphide challenge. *Int J Biochem Cell Biol*. 2017;83:1–14.
24. Mytych J, Wnuk M, Rattan SI. Low doses of nanodiamonds and silica nanoparticles have beneficial hormetic effects in normal human skin fibroblasts in culture. *Chemosphere*. 2016;148:307–315.
25. Haiss W, Thanh NT, Aveyard J, Fernig DG. Determination of size and concentration of gold nanoparticles from UV-vis spectra. *Anal Chem*. 2007;79(11):4215–4221.
26. Cybulsky MI, Iiyama K, Li H, et al. A major role for VCAM-1, but not ICAM-1, in early atherosclerosis. *J Clin Invest*. 2001;107(10):1255–1262.
27. Ross R. Atherosclerosis–an inflammatory disease. *N Engl J Med*. 1999;340(2):115–126.
28. Park YM, Febbraio M, Silverstein RL. CD36 modulates migration of mouse and human macrophages in response to oxidized LDL and may contribute to macrophage trapping in the arterial intima. *J Clin Invest*. 2009;119(1):136–145.
29. Park JG, Oh GT. The role of peroxidases in the pathogenesis of atherosclerosis. *BMB Rep*. 2011;44(8):497–505.
30. Boisselier E, Astruc D. Gold nanoparticles in nanomedicine: preparations, imaging, diagnostics, therapies and toxicity. *Chem Soc Rev*. 2009;38(6):1759–1782.
31. Leduc C, Si S, Gautier J, et al. A highly specific gold nanoprobe for live-cell single-molecule imaging. *Nano Lett*. 2013;13(4):1489–1494.
32. Mukherjee P, Bhattacharya R, Wang P, et al. Antiangiogenic properties of gold nanoparticles. *Clin Cancer Res*. 2005;11(9):3530–3534.
33. Chen YS, Hung YC, Liau I, Huang GS. Assessment of the in vivo toxicity of gold nanoparticles. *Nanoscale Res Lett*. 2009;4(8):858–864.
34. Connor EE, Mwamuka J, Gole A, Murphy CJ, Wyatt MD. Gold nanoparticles are taken up by human cells but do not cause acute cytotoxicity. *Small*. 2005;1(3):325–327.

35. King GL, Loeken MR. Hyperglycemia-induced oxidative stress in diabetic complications. *Histochem Cell Biol*. 2004;122(4):333–338.
36. Barathmanikanth S, Kalishwaralal K, Sriram M, et al. Anti-oxidant effect of gold nanoparticles restrains hyperglycemic conditions in diabetic mice. *J Nanobiotechnology*. 2010;8(1):16.
37. Shen K, Lu F, Xie J, et al. Cambogin exerts anti-proliferative and pro-apoptotic effects on breast adenocarcinoma through the induction of NADPH oxidase 1 and the alteration of mitochondrial morphology and dynamics. *Oncotarget*. 2016;7(31):50596–50611.
38. Bhattacharyya A, Chattopadhyay R, Mitra S, Crowe SE. Oxidative stress: an essential factor in the pathogenesis of gastrointestinal mucosal diseases. *Physiol Rev*. 2014;94(2):329–354.
39. Hamed S, Brenner B, Aharon A, Daoud D, Roguin A. Nitric oxide and superoxide dismutase modulate endothelial progenitor cell function in type 2 diabetes mellitus. *Cardiovasc Diabetol*. 2009;8(1):56.
40. Yakimovich NO, Ezhevskii AA, Guseinov DV, Smirnova LA, Gracheva TA, Klychkov KS. Antioxidant properties of gold nanoparticles studied by ESR spectroscopy. *Rus Chem Bull*. 2008;57(3):520–523.
41. Li L, Sawamura T, Renier G. Glucose enhances human macrophage LOX-1 expression: role for LOX-1 in glucose-induced macrophage foam cell formation. *Circ Res*. 2004;94(7):892–901.
42. Wang RC, Levine B. Autophagy in cellular growth control. *FEBS Lett*. 2010;584(7):1417–1426.
43. Ying L, Huang Y, Chen H, et al. Downregulated MEG3 activates autophagy and increases cell proliferation in bladder cancer. *Mol Biosyst*. 2013;9(3):407–411.
44. Ji Y, Di W, Yang Q, Lu Z, Cai W, Wu J. Inhibition of autophagy increases proliferation inhibition and apoptosis induced by the PI3K/mTOR inhibitor NVP-BEZ235 in breast cancer cells. *Clin Lab*. 2015;61(8):1043–1051.
45. Matus S, Castillo K, Hetz C. Hormesis: protecting neurons against cellular stress in Parkinson disease. *Autophagy*. 2012;8(6):997–1001.
46. Habib SL, Riley DJ, Mahimainathan L, Bhandari B, Choudhury GG, Abboud HE. Tuberin regulates the DNA repair enzyme OGG1. *Am J Physiol Renal Physiol*. 2008;294(1):F281–F290.
47. Nakagami H, Kaneda Y, Ogihara T, Morishita R. Endothelial dysfunction in hyperglycemia as a trigger of atherosclerosis. *Curr Diabetes Rev*. 2005;1(1):59–63.
48. Mariappan MM, Feliers D, Mummidi S, Choudhury GG, Kasinath BS. High glucose, high insulin, and their combination rapidly induce laminin-beta1 synthesis by regulation of mRNA translation in renal epithelial cells. *Diabetes*. 2007;56(2):476–485.

Supplementary materials

Table S1 Oligonucleotides used for quantitative real-time polymerase chain reaction

Gene	Primer	
iNOS (M)	FP	5′-TTCCAAGAGCCTTGATGTTT-3′
	RP	5′-GTAGGTAAGGGCGTTGGTCA-3′
iNOS (H)	FP	5′-CGTCTATGCGGGTTCAGTTG-3′
	RP	5′-TGCCTGTTTACCTCGCCTTA-3′
OGG1 (M)	FP	5′-GTGACTACGGCTGGCATCC-3′
	RP	5′-AGGCTTGGTTGGCGAAGG-3′
OGG1 (H)	FP	5′-GTG GAC TCC CAC TTC CAA GA-3′
	RP	5′-GAG ATG AGC CTC CAC CTC TG-3′
TNF-α (M)	FP	5′-CACACACACCCTCCTGATTG-3′
	RP	5′-CTCATTCAACCCTCGGAAAA-3′
IL-1-α (M)	FP	5′-AGAGCTTCCTGATGTGCCTT-3′
	RP	5′-CCCTCTTCTGGTGCTTCTGA-3′
ICAM (M)	FP	5′-ATCACATGGGTCGAGGGTTT-3′
	RP	5′-TAAGAAAGGGAGGTGCAGGG-3′
CX3CL-1 (M)	FP	5′-TCTGGTCCCAACTGCTGTAG-3′
	RP	5′-TCACTGGGGTTGAGTCATCC-3′
CXCL-10 (M)	FP	5′-AGTCAGGAGAAAGGGCGAAA-3′
	RP	5′-GAGAGACGCATCCCATCGTA-3′
CCL-8 (M)	FP	5′-TTTTCCAGGAGCTCAGAGGG-3′
	RP	5′-CTTGCTCCAGAGGTGAAGGA-3′
Mn-SOD (M)	FP	5′-ATGTTGTGTCGGGCGGCG-3′
	RP	5′-AGGTAGTAAGCGTGCTCCCACACG-3′
Cu-Zn-SOD (M)	FP	5′-AAGGCCGTGTGCGTGCTGAA-3′
	RP	5′-CAGGTCTCCAACATGCCTCT-3′
Catalase (M)	FP	5′-GCAGATACCTGTGAACTGTC-3′
	RP	5′-GTAGAATGTCCGCACCTGAG-3′
GPx (M)	FP	5′-CCTCAAGTACGTCCGACCTG-3′
	RP	5′-CAATGTCGTTGCGGCACACC-3′
MMP-2 (M)	FP	5′-TTGACGGTAAGGACGGACTC-3′
	RP	5′-ACTTGCAGTACTCCCCATCG-3′
MMP-9 (M)	FP	5′-TTGACAGCGACAAGAAGTGG-3′
	RP	5′-CCCTCAGTGAAGCGGTACAT-3′
GAPDH (M)	FP	5′-GAGAGGCCCTATCCCAACTC-3′
	RP	5′-TTCACCTCCCCATACACACC-3′
GAPDH (H)	FP	5′-AGCCACATCGCTCAGACAC-3′
	RP	5′-GCCCAATACGACCAAATCC-3′

Abbreviations: FP, forward primer; H, human; M, mouse; RP, reverse primer.

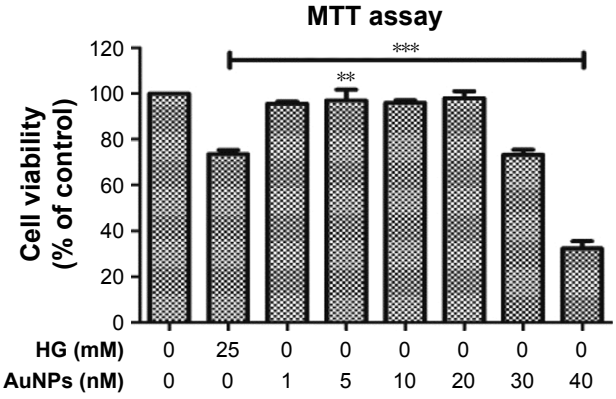

Figure S1 Dose dependent effect of AuNPs on HG-induced apoptosis in macrophage cells.
Note: **$P<0.01$; ***$P<0.001$.
Abbreviations: AuNPs, gold nanoparticles; HG, high glucose.

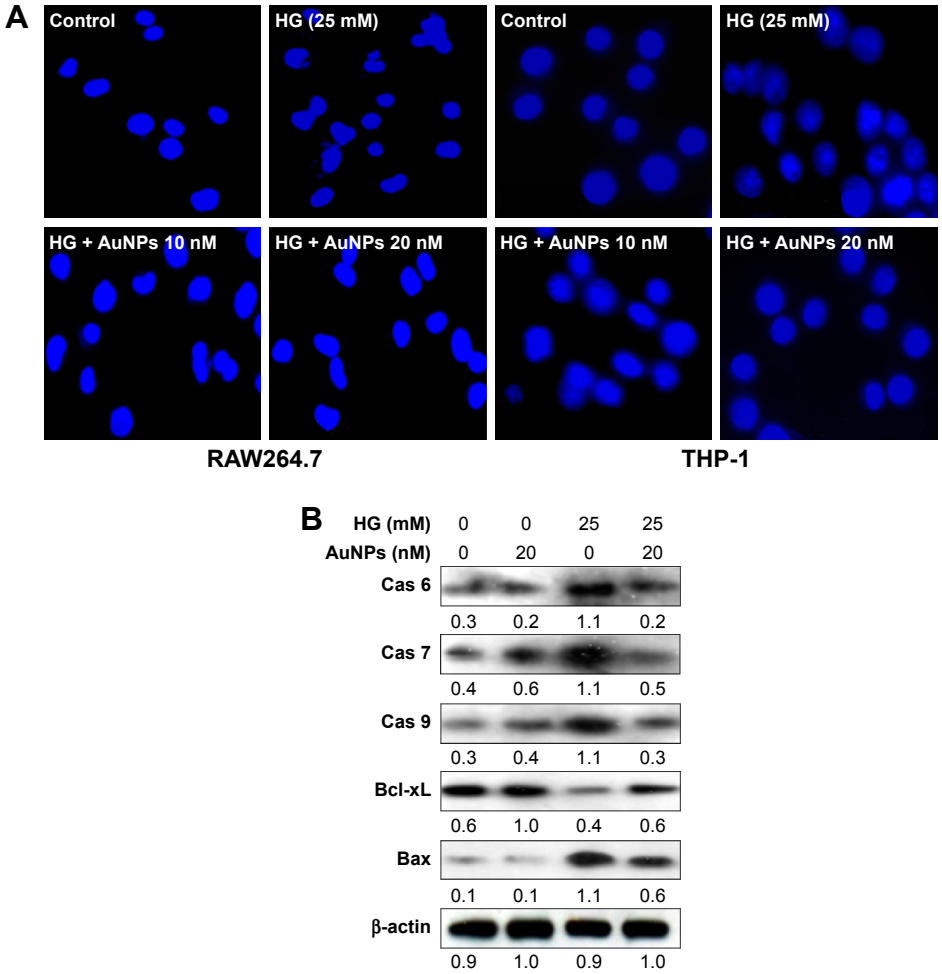

Figure S2 Effect of AuNPs on HG-induced apoptosis in macrophage cells.
Notes: (**A**) Hoechst nuclear staining with/without treatment of AuNPs in HG condition for 24 h. Magnification 40×. (**B**) A representative immunoblot analysis of apoptotic markers such as caspases, Bcl.xL and BAX, with/without treatment of AuNPs only in control group in HG condition for 24 h.
Abbreviations: AuNPs, gold nanoparticles; HG, high glucose.